Adrenomedullin Enhances Therapeutic Potency of Mesenchymal Stem Cells After Experimental Stroke in Rats

Kenichiro Hanabusa, MD; Noritoshi Nagaya, MD; Takashi Iwase, MD; Takefumi Itoh, MD; Shinsuke Murakami, MD; Yoshito Shimizu, MD; Waro Taki, MD; Kunio Miyatake, MD; Kenji Kangawa, PhD

Background and Purpose—Adrenomedullin (AM) induces angiogenesis and inhibits cell apoptosis through the phosphatidylinositol 3-kinase/Akt pathway. Transplantation of mesenchymal stem cells (MSCs) has been shown to improve neurological deficits after stroke in rats. We investigated whether AM enhances the therapeutic potency of MSC transplantation.

Methods—Male Lewis rats (n=100) were subjected to 2-hour middle cerebral artery occlusion. Immediately after reperfusion, rats were assigned randomly to receive intravenous transplantation of MSCs plus subcutaneous infusion of AM for 7 days (MSC+AM group), AM infusion alone (AM group), MSC transplantation alone (MSC group), or vehicle infusion (control group). Neurological and immunohistological assessments were performed to examine the effects of these treatments.

Results—Some engrafted MSCs were positive for neuronal and endothelial cell markers, although the number of differentiated MSCs did not differ significantly between the MSC and MSC+AM groups. The neurological score significantly improved in the MSC, AM, and MSC+AM groups compared with the control group. Importantly, improvement in the MSC+AM group was significantly greater than that in the MSC and AM groups. There was marked induction of angiogenesis in the ischemic penumbra in the MSC+AM group, followed by the AM, MSC, and control groups. AM infusion significantly inhibited apoptosis of transplanted MSCs. As a result, the number of engrafted MSCs in the MSC+AM group was significantly higher than that in the MSC group.

Conclusions—AM enhanced the therapeutic potency of MSCs, including neurological improvement, possibly through inhibition of MSC apoptosis and induction of angiogenesis. (***Stroke.*** **2005;36:853-858.)**

Key Words: angiogenesis ■ apoptosis ■ stroke

Despite the advances in medical and surgical treatment, stroke is still a major cause of morbidity and mortality. Mesenchymal stem cells (MSCs) are multipotent, and some transplanted MSCs can differentiate into neuronal cells and endothelial cells in the recipient brain.[1] A recent study has shown that MSCs have ability to pass blood–brain barrier, particularly in injury sites.[1–3] In addition, transplantation of MSCs into the brain of experimental stroke animals has been shown to improve neurological functional recovery.[1,3] The effect of MSC transplantation is dependent on the number of transplanted MSCs.[1] However, the viability of MSCs after transplantation is relatively poor.[4] Thus, a new approach to augment the effect of MSC transplantation is desirable for the application of MSC therapy to the regenerative treatment of stroke.

Adrenomedullin (AM) is a potent vasodilatory peptide that was originally isolated from human pheochromocytoma.[5] Recent study has shown that intramuscular administration of AM DNA induces therapeutic angiogenesis in a hindlimb ischemic model via activation of Akt.[6] In addition, AM has been shown to exert antiapoptotic effects on a variety of cells.[7] We also demonstrated antiapoptotic effects of AM in myocardial ischemia/reperfusion injury through the phosphatidylinositol 3-kinase (PI3K)/Akt pathway.[8] These results suggest that AM may play an important role in induction of angiogenesis and inhibition of apoptosis. Taking these findings together, AM infusion may have additive or synergetic effects on MSC transplantation, which may result in improvement of neurological functional recovery. Thus, the purpose of this study was to investigate whether combined therapy of AM infusion and MSC transplantation significantly improves neurological functional recovery compared with MSC transplantation alone.

Received December 7, 2004; accepted January 6, 2005.

From the Department of Regenerative Medicine and Tissue Engineering (K.H., N.N., T. Iwase, T. Itoh, S.M., Y.S.), National Cardiovascular Center Research Institute, Osaka, Japan; Department of Neurosurgery (K.H., W.T.), Mie University School of Medicine, Mie, Japan; Department of Internal Medicine (K.M.), National Cardiovascular Center, Osaka, Japan; and Department of Biochemistry (K.K.), National Cardiovascular Center Research Institute, Osaka, Japan.

Reprint requests to Noritoshi Nagaya, MD, Department of Regenerative Medicine and Tissue Engineering, National Cardiovascular Center Research Institute, 5-7-1 Fujishirodai, Suita, Osaka 565-8565, Japan. E-mail nnagaya@ri.ncvc.go.jp

Stroke is available at http://www.strokeaha.org

DOI: 10.1161/01.STR.0000157661.69482.76

Materials and Methods

Stroke Model

Male Lewis rats (Japan SLC, Hamamatsu, Japan) weighing 230 to 260 g were used in all experiments. Middle cerebral artery occlusion (MCAO) was performed by an intraluminal thread as described previously.[2] The animal care committee of the National Cardiovascular Center approved this experimental protocol.

MSC Preparation

MSC expansion was performed according to a previously described method.[9] In brief, we euthanized male Lewis rats and harvested bone marrow. Bone marrow cells were introduced into 100-mm dishes and cultured in α-minimum essential medium (MEN) supplemented with 10% FBS. After nonadherent hematopoietic cells were removed with medium replacement, spindle-shaped adherent cells developed visible symmetric colonies by day 5 to 7. They were expanded to >50 million cells, ≈4 to 5 passages. These adherent cells were collected with 0.05% trypsin and 2% EDTA (GIBCO) for 3 minutes at 37°C. These cells were analyzed by fluorescence-activated cell sorting as described previously.[10] Most of cultured adherent cells were positive for CD29 (98±1%) and CD90 (99±1%) and negative for CD34 (2±1%) and CD45 (1±1%). We confirmed that major population of the adherent cells were MSCs. MSCs secreted a large amount of an antiapoptotic and angiogenic factor, including vascular endothelial growth factor (VEGF; 960±14 pg/10^6 cells), 24 hours after culture.

MSC Transplantation and AM Infusion

Immediately after 2-hour MCAO, rats were assigned randomly to the following 4 groups. (1) PBS injection plus vehicle infusion (control group n=22); (2) MSC injection plus vehicle infusion (MSC group n=28); (3) PBS injection and AM infusion (AM group n=22); and (4) MSC injection plus AM infusion (MSC+AM group n=28). MSCs (1×10^6 cells) suspended in PBS were injected via a tail vein. Four rats underwent a sham operation without an intraluminal thread. AM (0.05 μg/kg per minute) or vehicle was infused for 7 days using a mini-osmotic pump (Alzet) implanted in the posterior cervical subcutaneous region. The dose of AM used in this study has antiapoptotic effects without significant hypotension.[8]

Detection of MSC Differentiation in Ischemic Hemisphere

Red fluorescent-labeled MSCs were transplanted to examine MSC differentiation as described previously.[11] In brief, suspended MSCs were labeled with fluorescent dye (PKH26 Red Fluorescent Cell Linker Kit; Sigma). Three minutes after labeling, FBS was added for 1 minute to stop reaction and cells were washed by PBS. A recent study has shown that the sensitivity and specificity for cell labeling with PKH26 are ≈100%, and transplanted cells are detectable at least up to 4 months after transplantation in the host brain.[11] Rats were euthanized with an overdose of pentobarbital on day 14 after MCAO. For preparation of frozen sections, rats were perfused transcardially with normal saline and the brain was removed immediately. Blocks corresponding to coronal coordinates for bregma −1 to 1 mm were obtained and frozen rapidly in liquid nitrogen. A series of 6-μm-thick sections was obtained. Numbers of PKH26-positive cells were counted in a blind fashion and expressed as the average in 5 sections. To detect the differentiation of MSCs, immunohistochemical staining was performed. Sections were incubated with anti-von Willebrand factor (vWF) polyclonal antibody (1:200; DAKO, Glostrup, Denmark), rabbit anti-glial fibrillary acidic protein (GFAP; 1:500; DAKO), and mouse anti-neuronal nuclei marker (NeuN; 1:200; Chemicon, Hampshire, UK), followed by incubation with fluorescein isothiocynate (FITC)–conjugated rabbit immunoglobulin antibody (DAKO) and FITC-conjugated mouse immunoglobulin antibody (BD Pharmingen, San Diego, Calif), respectively.

Neurological Assessment

Neurological assessment was performed on days 1, 7, and 14 using a modified neurological severity score, as described previously.[1] In brief, this score is derived by evaluating animals for hemiparesis (response to raising the rat by the tail or placing the rat on a flat surface), sensory deficits (placing, proprioception), beam balance tests (response to placement and posture on a narrow beam and time before dropping), absent reflexes (pinna, corneal, startle), and abnormal movement (seizure, myoclonus, myodystony). One point is awarded for the inability to perform a task or for the lack of a tested reflex.

Measurement of Infarct Size

Rats were euthanized on day 1 (each group n=8) and on day 14 (each group n=8). For preparation of paraffin-embedded sections, rats were perfused transcardially with 4% paraformaldehyde. Brains were cut into 7 equally spaced (2 mm) coronal blocks, and each section was stained with hematoxylin and eosin. Infarct size was determined by the "indirect method," as described previously,[1] and expressed as a percentage of the intact contralateral hemispheric size.

Assessment of Angiogenesis

Angiogenesis was analyzed on day 14 (each group n=8). Paraffin sections corresponding to coronal coordinates for bregma −1 to 1 mm were selected. Sections were incubated with anti-vWF antibody and then incubated with biotinylated anti-rabbit immunoglobulin and with streptoavidin-horseradish peroxidase (HRP) complex (DAKO). The HRP reaction was detected in diaminobenzidine (DAB). To quantify angiogenesis, 8 fields of view from the ischemic penumbra and contralateral noninfarct tissue were randomly selected as described previously,[2] and images (×100 magnification) were acquired using a microscope (ZWISS AXIOVERT 135) and a digital camera (ZWISS AXIO cam). The vWF-immunoreactive area in each image was determined by image analysis using software (Win Roof 5.0; Microsoft) as described previously.[12] The values corresponding to total brown areas were averaged and expressed as the mean percentage of stained vessel area per 100 μm^2. To detect newly formed vessels, tissue sections were stained for Ki67, a marker for cell proliferation, with the use of monoclonal anti-Ki67 antibody (DAKO). The numbers of Ki67-positive microvessels were counted and expressed the average in 8 fields.

Detection of Apoptosis in Ischemic Penumbra

The antiapoptotic effects of AM on the ischemic penumbra were examined 24 hours after MCAO (each group n=8). Paraffin-embedded sections were prepared for TUNEL assay. TUNEL staining was performed with a commercially available kit (ApopTag Plus; Serological Corporation). The numbers of TUNEL-positive cells per field were counted and expressed as the average in 8 fields. To evaluate apoptosis of transplanted MSCs in the ischemic brain, an additional 12 rats (MSC group n=6; MSC+AM group n=6) were euthanized on day 3. Frozen sections were used for TUNEL staining (ApopTag Fluorescein kit). The numbers of TUNEL- and PKH26-positive cells were counted and expressed as the average in 5 sections.

Statistical Analysis

All data were expressed as mean±SEM. Student's unpaired t test was used to compare differences between 2 groups. Comparisons of parameters among 4 groups were made by 1-way ANOVA, followed by Newman–Keuls test. Comparisons of the time course of neurological scores were made by 2-way ANOVA for repeated measures, followed by Newman–Keuls test. A P value <0.05 was considered statistically significant.

Results

Engraftment and Differentiation of Transplanted MSCs

Intravenously administered MSCs were engrafted in the ischemic penumbra. Some MSCs were positive for NeuNs and GFAP (Figure 1A and 1B). Other MSCs were positive for

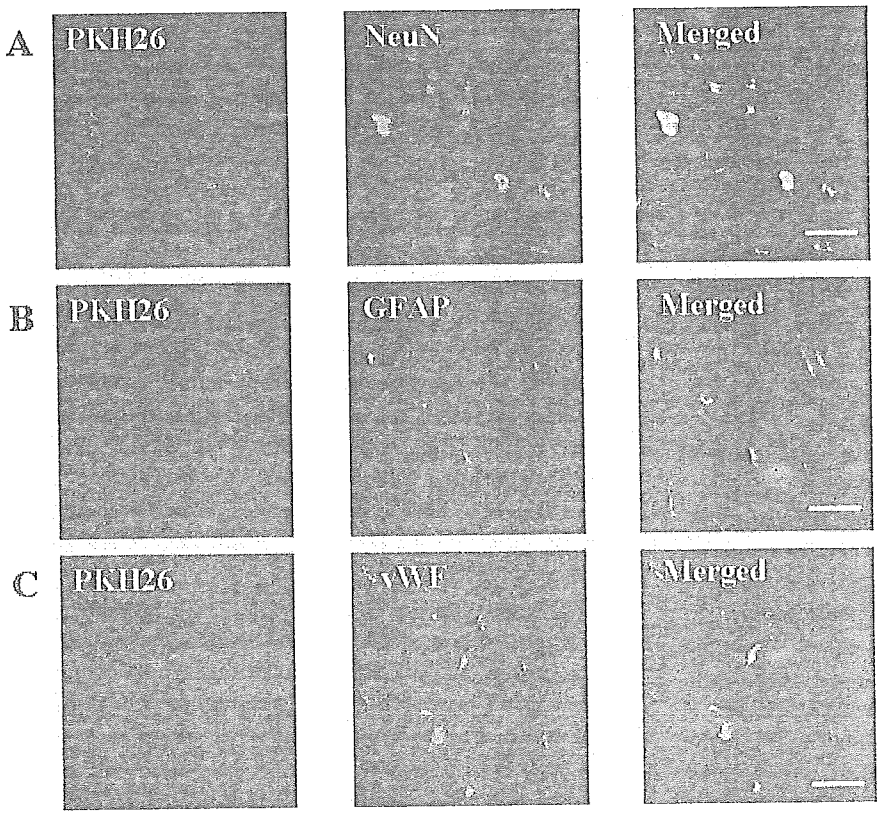

Figure 1. Engraftment and differentiation of transplanted MSCs. PKH26-labeled MSCs were frequently observed in ischemic penumbra. Some PKH26-positive MSCs (red) expressed neuronal marker (NeuN; green; A), astrocyte marker (GFAP; green; B), or endothelial cell marker (vWF; green; C). Bars=20 μm.

vascular endothelial marker vWF (Figure 1C). The numbers of differentiated MSCs did not differ significantly between the MSC and MSC+AM groups (data not shown). Few MSCs were observed in the contralateral nonischemic tissue.

Neurological Assessment

Neurological severity scores on day 1 did not differ significantly among 4 groups (Figure 2). Neurological deficits gradually improved in all groups. Scores in the MSC and AM groups on days 7 and 14 were lower than those in the control group ($P<0.05$), although there were no significant differences between the AM and MSC groups on days 7 and 14. Interestingly, the scores on days 7 and 14 were lowest in the MSC+AM group among the 4 groups.

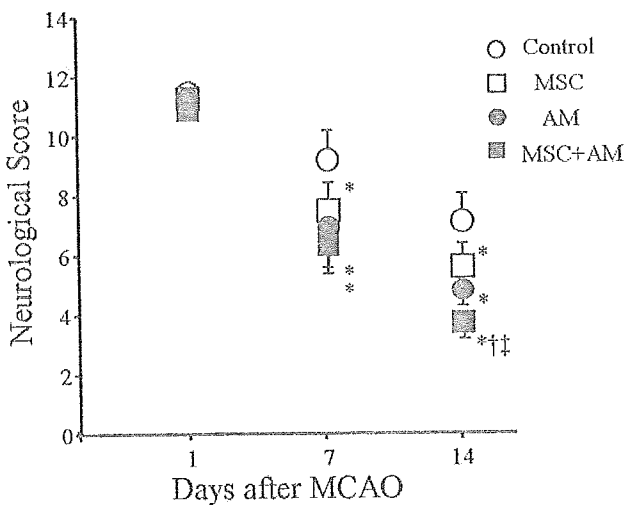

Figure 2. Neurological score on days 1, 7, and 14 in the control group, MSC group, AM group, and MSC+AM group. Data are mean±SEM. *$P<0.05$ vs control group; †$P<0.05$ vs MSC group; ‡$P<0.05$ vs AM group.

Infarct Size and Physiological Data

Infarct size on day 1 in the MSC or AM group was significantly smaller than that in the control group ($P<0.05$; Table 1). Furthermore, the infarct size in the MSC+AM group was the smallest among 4 groups. However, on day 14, there was no significant difference in infarct size, although the infarct size tended to be small in the treatment groups. Percent increase in body weight in the MSC, AM, and MSC+AM groups was higher than that in the control group ($P<0.05$; Table 2).

TABLE 1. Percent Infarct Size to the Contralateral Hemisphere

		Infarct Size (%)	
Group	No.	Day 1	Day 14
Control	8	31±1	31±2
MSC	8	27±1*	29±2
AM	8	28±1*	29±1
MSC+AM	8	25±1*†‡	28±2

Control indicates rats given vehicle infusion; MSC, rats given MSC transplantation; AM, rats given AM infusion; MSC+AM, rats given MSC transplantation and AM infusion.

Data are mean±SEM.

*$P<0.05$ vs control group.

†$P<0.05$ vs MSC group.

‡$P<0.05$ vs AM group.

TABLE 2. Percent Increase of Body Weight

Group	No.	% Increase of Body Weight
Control	16	8±3
MSC	16	12±2*
AM	16	13±2*
MSC+AM	16	14±2*

Control indicates rats given vehicle infusion; MSC, rats given MSC transplantation; AM, rats given AM infusion; MSC+AM, rats given MSC transplantation and AM infusion.

Data are mean±SEM.

*$P<0.05$ vs control group.

Angiogenic Potency of AM and MSCs

Angiogenesis in the ischemic penumbra was observed after MCAO compared with sham operation (Figure 3A). Furthermore, MSC transplantation or AM infusion induced angiogenesis in the ischemic penumbra, and particularly, the angiogenic effect was marked after combined therapy of MSCs and AM. Quantitative analysis demonstrated that the area of vWF staining in the MSC and AM groups was higher than that in the control group ($P<0.05$ versus control group; Figure 3B). There was no significant difference between the MSC and AM groups. Interestingly, the area of vWF staining in the MSC+AM group was highest among the 4 groups ($P<0.05$ versus MSC and AM groups). There were no significant differences in neovascularization of noninfarct tissue in all groups (Figure 3A and 3B). Representative photomicrographs of immunostaining of Ki67, a marker for cell proliferation, demonstrated that AM infusion and MSC transplantation increased the number of Ki67-positive newly formed microvessels in the ischemic penumbra (Figure 3C and 3D).

Antiapoptotic Effects of AM on Neuronal Cells and Transplanted MSCs

TUNEL-positive cells were frequently observed in the ischemic penumbra on day 1 (Figure 4A). Quantitative analysis demonstrated that the number of TUNEL-positive cells in the treatment groups was lower than that in the control group ($P<0.05$ versus control group; Figure 4B). Interestingly, the number of TUNEL-positive cells in the MSC+AM group was significantly lower than that in the MSC and AM groups ($P<0.05$ versus MSC and AM groups), although there was no significant difference between the MSC and AM groups.

The majority of transplanted MSCs were positive for TUNEL staining on day 3 (Figure 5A). Infusion of AM decreased TUNEL-positive MSCs in the ischemic penumbra. Quantitative analysis demonstrated that the number of apoptotic MSCs in the MSC+AM group was significantly lower than that in the MSC group ($P<0.05$; Figure 5B). As a result, the number of engrafted MSCs in the MSC+AM group on day 14 was markedly higher than that in the MSC group ($P<0.05$; Figure 5C). The number of TUNEL-positive non-

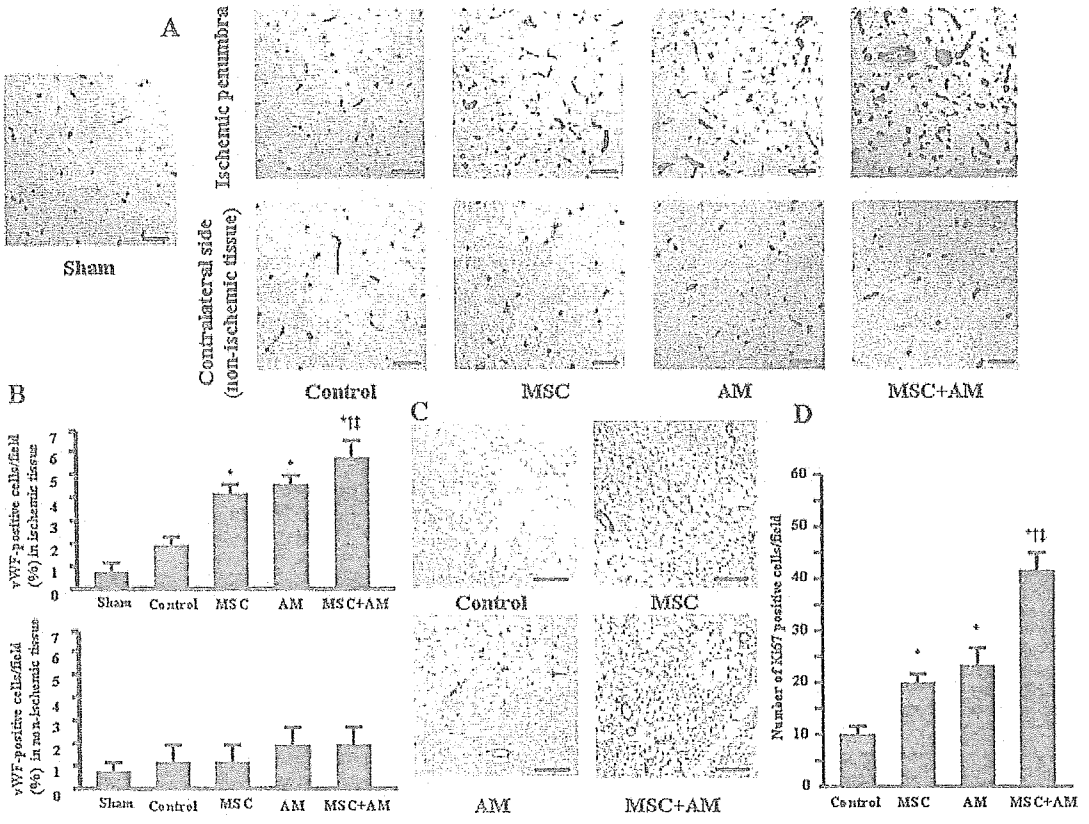

Figure 3. A, Representative photomicrographs of vWF staining in ischemic penumbra (top) and in contralateral nonischemic tissue (bottom). Bars=25 μm. B, Quantitative analysis of angiogenesis using the area of vWF staining in ischemic penumbra (top) and in nonischemic tissue (bottom). C, Representative photomicrographs of Ki67 staining. Bars=50 μm. D, Quantitative analysis of the number of Ki67-positive microvessels. Data are mean±SEM. *$P<0.05$ vs control group; †$P<0.05$ vs MSC group; ‡$P<0.05$ vs AM group.

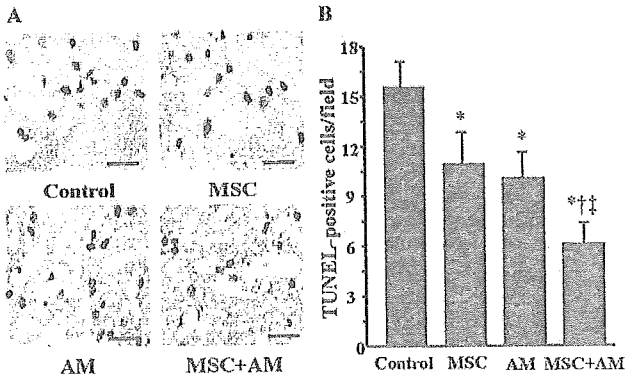

Figure 4. A, Representative photomicrographs of TUNEL staining in ischemic penumbra. The number of TUNEL-positive cells (DAB; brown) in the MSC+AM group was markedly lower than that in the other 3 groups. B, Quantitative analysis of the number of TUNEL-positive cells. Data are mean±SEM. *P<0.05 vs control group; †P<0.05 vs MSC group; ‡P<0.05 vs AM group. Bars=20 μm.

MSCs, including neuronal cells, was also decreased by AM infusion (Figure 5D).

Discussion

In the present study, we demonstrated that: (1) AM infusion or MSC transplantation induced angiogenesis and inhibited apoptosis of neuronal cells in the ischemic penumbra; (2) infusion of AM enhanced the angiogenic potency and antiapoptotic effects of MSC transplantation; (3) AM inhibited apoptosis of transplanted MSCs themselves and increased the number of engrafted MSCs; and (4) combination therapy of AM and MSC induced greater improvement in neurological functions than AM infusion or MSC transplantation alone.

Endogenous AM has been shown to be upregulated by hypoxia in the ischemic brain through a compensatory mechanism.[13] A previous report has demonstrated that pretreatment with AM reduces brain injury and improves neurological deficits in a rat stroke model.[14] The present study demonstrated that AM infusion after the onset of stroke improved neurological functions in rats. However, the underlying mechanisms still remain unclear. We have shown that intramuscular administration of AM DNA induces therapeutic angiogenesis in a hindlimb ischemic model via activation of Akt.[6] Expectedly, in the present study, infusion of AM induced neovascularization in the ischemic penumbra. On the other hand, AM has been shown to have potent antiapoptotic effects on various cells through the PI3K/Akt pathway.[7,8] Interestingly, in the present study, short-term infusion of AM markedly decreased TUNEL-positive cells in the ischemic penumbra. AM infusion significantly decreased infarct size on day 1, although the significant change was not observed on day 14. These results suggest that AM improves neurological functions, at least in part, through induction of angiogenesis and inhibition of neuronal cell apoptosis in the ischemic penumbra.

Recently, transplantation of MSCs has been shown to improve neurological functions in experimental stroke.[1,3] The beneficial effects are considered to be mediated by increases in endogenous angiogenic and antiapoptotic factors including VEGF, a potent neuroprotective factor,[12] and by differentiation of MSCs themselves into neuronal cells.[1] The present study showed that MSCs secreted a large amount of VEGF. In fact, we demonstrated in vivo that MSCs induced angiogenesis and inhibited cell apoptosis in the ischemic penumbra (Figures 3 and 4). Furthermore, some transplanted MSCs differentiated into neuronal cells and endothelial cells. Thus, MSCs have neuroprotective effects not only through their differentiation, but also through their ability to secret angiogenic and antiapoptotic factors. Nevertheless, the majority of transplanted MSCs were positive for TUNEL staining on day 3. Interestingly, infusion of AM significantly decreased the

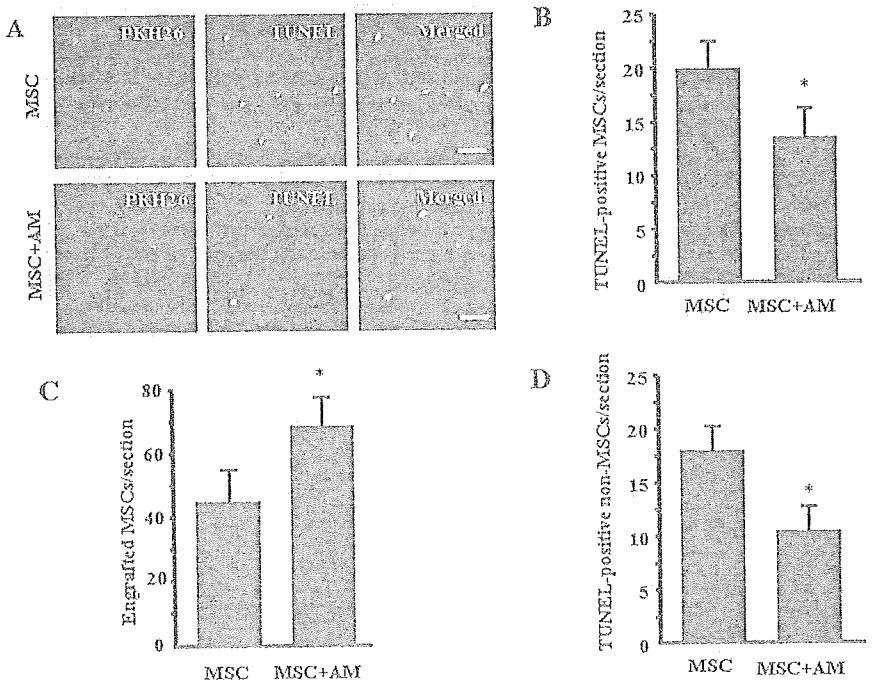

Figure 5. A, Representative photomicrographs of MSC apoptosis after transplantation. Transplanted MSCs were labeled with PKH26. TUNEL-positive cells (green) were frequently observed in ischemic penumbra. Infusion of AM decreased TUNEL-positive MSCs (double-positive cells, merged). B, Quantitative analysis of the number of TUNEL-positive MSCs on day 3. C, The number of engrafted MSCs on day 14. D, Quantitative analysis of the number of TUNEL-positive non-MSCs. Data are mean±SEM. *P<0.05. Bars=100 μm.

number of apoptotic cells on day 3. The number of engrafted MSCs in the MSC+AM group on day 14 was markedly higher than that in the MSC group. These results suggest that AM contributes to prolonging the viability of transplanted MSCs. In addition, AM inhibited apoptosis of non-MSCs, suggesting direct protective effects of AM on the ischemic penumbra. Furthermore, a combination of AM infusion and MSC transplantation markedly improved neurological functions compared with MSC transplantation or AM infusion alone. The infarct size on day 1 was smallest in the MSC+AM group, although infarct size on day 14 in the MSC+AM group tended to be small compared with that in other groups. Considering the angiogenic and antiapoptotic effects of AM and MSCs, administered AM may have additional or synergetic effects on MSC transplantation, leading to further improvement in neurological functions after stroke. Interestingly, a significant increase in body weight was observed in rats with low neurological score after treatment. A previous report has shown that body weight after stroke was higher in bFGF-treated rats than in vehicle-treated rats.[15] These results suggest that earlier recovery of neurological deficits might have restored impaired food intake after stroke.

MSC transplantation to treat brain ischemia has been investigated recently. We demonstrated previously the safety of AM infusion in patients with congestive heart failure.[16] Thus, combination therapy using AM infusion and MSC transplantation may be a novel and promising therapeutic strategy for treatment of stroke. However, systemically administered MSCs and AM may develop cancer and retinopathy via their angiogenic potential. Further studies are necessary to examine the safety and efficacy of this treatment.

In conclusion, AM enhanced the therapeutic potency of MSCs, including neurological improvement, possibly through inhibition of MSC apoptosis and induction of angiogenesis. A combination of AM infusion and MSC transplantation may be a new therapeutic strategy for treatment of stroke.

Acknowledgments

This work was supported by the Research Grant for Cardiovascular Disease (16C-6) from the Ministry of Health, Labour and Welfare; Industrial Technology Research Grant Program in 2003 from New Energy and Industrial Technology Development Organization of Japan; Health and Labor Sciences Research grants (H16-trans-008); and the Promotion of Fundamental Studies in Health Science of the Organization for Pharmaceutical Safety and Research of Japan.

References

1. Chen J, Li Y, Wang L, Zhang Z, Lu D, Lu M, Chopp M. Therapeutic benefit of intravenous administration of bone marrow stromal cells after cerebral ischemia in rats. *Stroke*. 2001;32:1005–1011.
2. Chen J, Zhang ZG, Li Y, Wang L, Xu YX, Gautam SC, Lu M, Zhu Z, Chopp M. Intravenous administration of human bone marrow stromal cells induces angiogenesis in the ischemic boundary zone after stroke in rats. *Circ Res*. 2003;92:692–699.
3. Chopp M, Li Y. Treatment of neural injury with marrow stromal cells. *Lancet Neurol*. 2002;1:92–100.
4. Mangi AA, Noiseux N, Kong D, He H, Rezvani M, Ingwall JS, Dzau VJ. Mesenchymal stem cells modified with Akt prevent remodeling and restore performance of infarcted hearts. *Nat Med*. 2003;9:1195–1201.
5. Kitamura K, Kangawa K, Kawamoto M, Ichiki Y, Nakamura S, Matsuo H, Eto T. Adrenomedullin: a novel hypotensive peptide isolated from human pheochromocytoma. *Biochem Biophys Res Commun*. 1993;192:553–560.
6. Tokunaga N, Nagaya N, Shirai M, Tanaka E, Ishibashi-Ueda H, Harada-Shiba M, Kanda M, Ito T, Shimizu W, Tabata Y, Uematsu M, Nishigami K, Sano S, Kangawa K, Mori H. Adrenomedullin gene transfer induces therapeutic angiogenesis in a rabbit model of chronic hind limb ischemia: benefits of a novel nonviral vector, gelatin. *Circulation*. 2004;109:526–531.
7. Kato H, Shichiri M, Marumo F, Hirata Y. Adrenomedullin as an autocrine/paracrine apoptosis survival factor for rat endothelial cells. *Endocrinology*. 1997;138:2615–2620.
8. Okumura H, Nagaya N, Itoh T, Okano I, Hino J, Mori K, Tsukamoto Y, Ishibashi-Ueda H, Miwa S, Tambara K, Toyokuni S, Yutani C, Kangawa K. Adrenomedullin infusion attenuates myocardial ischemia/reperfusion injury through the phosphatidylinositol 3-kinase/Akt-dependent pathway. *Circulation*. 2004;109:242–248.
9. Pittenger MF, Mackay AM, Beck SC, Jaiswal RK, Douglas R, Mosca JD, Moorman MA, Simonettii DW, Craig S, Marshak DR. Multilineage potential of adult human mesenchymal stem cell. *Science*. 1999;284:143–147.
10. Nagaya N, Fujii T, Iwase T, Ohgushi H, Itoh T, Uematsu M, Yamagishi M, Mori H, Kangawa K, Kitamura S. Intravenous administration of mesenchymal stem cells improves cardiac function in rats with acute myocardial infarction through angiogenesis and myogenesis. *Am J Physiol Heart Circ Physiol*. 2004;287:H2670–H2676.
11. Jean S, Haas P, Bauer P, Rolfs A, Wree A. Immunocytochemical characterization of in vitro PKH26-labelled and intracerebrally transplanted neonatal cells. *Acta Histochem*. 2000;102:273–280.
12. Sun Y, Jin K, Xie L, Childs J, Mao XO, Logvinova A, Greenberg DA. VEGF-induced neuroprotection, neurogenesis, and angiogenesis after focal cerebral ischemia. *J Clin Invest*. 2003;111:1843–1851.
13. Serrano J, Alonso D, Encinas JM, Lopez JC, Fernandez AP, Castro-Blanco S, Fernandez-Vizarra P, Richart A, Bentura ML, Santacana M, Uttenthal LO, Cuttitta F, Rodrigo J, Martinez A. Adrenomedullin expression is up-regulated by ischemia-reperfusion in the cerebral cortex of the adult rat. *Neuroscience*. 2002;109:717–731.
14. Watanabe K, Takayasu M, Noda A, Hara M, Takagi T, Suzuki Y, Yoshia J. Adrenomedullin reduces ischemic brain injury after transient middle cerebral artery occlusion in rats. *Acta Neurochir (Wien)*. 2001;143:1157–1161.
15. Jiang N, Finklestein SP, Do T, Caday CG, Charette M, Chopp M. Delayed intravenous administration of basic fibroblast growth factor (bFGF) reduces infarct volume in a model of focal cerebral ischemia/reperfusion in the rat. *J Neurol Sci*. 1996;139:173–179.
16. Nagaya N, Satoh T, Nishikimi T, Uematsu M, Furuichi S, Sakamaki F, Oya H, Kyotani S, Nakanishi N, Goto Y, Masuda Y, Miyatake K, Kangawa K. Hemodynamic, renal, and hormonal effects of adrenomedullin infusion in patients with congestive heart failure. *Circulation*. 2000;101:498–503.

0013-7227/05/$15.00/0
Printed in U.S.A.

Endocrinology 146(6):2709–2715

doi: 10.1210/en.2004-0645

Developmental Changes in the Pattern of Ghrelin's Acyl Modification and the Levels of Acyl-Modified Ghrelins in Murine Stomach

Yoshihiro Nishi, Hiroshi Hiejima, Hiroharu Mifune, Takahiro Sato, Kenji Kangawa, and Masayasu Kojima

Molecular Genetics, Institute of Life Science (Y.N., H.H., T.S., M.K.), and Institute of Animal Experimentation (H.M.), Kurume University, Fukuoka 839-0861; and Department of Biochemistry, National Cardiovascular Center Research Institute (K.K.), Osaka 565-8565, Japan

Ghrelin is an acylated peptide hormone secreted primarily from endocrine cells in the stomach. The major active form of ghrelin is a 28-amino acid peptide with an *n*-octanoyl modification at Ser^3 (*n*-octanoyl ghrelin), which is essential for its activity. In addition to *n*-octanoyl ghrelin, other forms of ghrelin peptide exist, including *des*-acyl ghrelin, which lacks an acyl modification, and other minor acylated ghrelin species, such as *n*-decanoyl ghrelin, whose Ser^3 residue is modified by *n*-decanoic acid. Multiple reports have identified various physiological functions of ghrelin. However, until now, there have been no reports that explore the process of ghrelin acyl modification, and only a few studies have compared the levels of des-acyl, *n*-octanoyl, and/or other minor populations of acylated ghrelin peptides. In this study we report that the amount of *n*-octanoyl ghrelin in murine stomachs increases gradually during the suckling period to a maximal level at 3 wk of age and falls sharply after the initiation of weaning. However, the concentration (picomoles per milligram of wet weight tissue) of total ghrelin, which includes *des*-acyl and all acylated forms of ghrelin peptides with intact C termini in murine stomach, remains unchanged across this suckling-weaning transition. Prematurely weaned mice exhibited a significant decrease in the amount of *n*-octanoyl or *n*-decanoyl ghrelin in the stomach. Orally ingested glyceryl trioctanoate, a medium-chain triacylglyceride rich in milk lipids, significantly increased the level of *n*-octanoyl-modified ghrelin in murine stomach. Fluctuations in the proportion of this biologically active, acyl-modified ghrelin could contribute to or be influenced by the change in energy metabolism during the suckling-weaning transition. (*Endocrinology* 146: 2709–2715, 2005)

GHRELIN IS AN endogenous ligand for the GH secretagogue (GHS) receptor (GHS-R) (1, 2). GHSs are synthetic substances with potent GH-releasing activity (3–5). Although ghrelin was initially purified from the stomach, it is also expressed in the brain, pancreas, small intestine, and other tissues (6). In addition to its potent GH-releasing activity (1), ghrelin stimulates appetite and influences adiposity (7, 8). The third amino acid residue of ghrelin, a serine (Ser^3), is modified by an acyl group; this modification is essential for ghrelin's biological activity through the classical ghrelin receptor, GHS-R1a (1, 9). Although the primary acyl chain modifying ghrelin molecules in humans and rodents is an *n*-octanoyl group (C8:0, an eight-carbon chain containing no double bonds) (1, 10), different acyl groups modify a minor population of ghrelin peptides. These acyl groups include *n*-decanoyl (C10:0, a 10-carbon chain lacking double bonds) and *n*-decenoyl (C10:1, a 10-carbon chain containing one double bond) (11–13). To our knowledge, the acyl modification of ghrelin is the first known example of a fatty acid modification of a peptide hormone.

A number of reports have been published on the regulation of ghrelin secretion in the context of energy metabolism that did not distinguish between acyl-modified and *des*-acyl ghrelin (14–18). However, there have been only a few reports comparing the levels of *n*-octanoyl, des-acyl, and/or total ghrelin, the last of which encompasses *des*-acyl and all acyl-modified ghrelin peptides with intact C termini (19, 20).

In this study we measured the amount of *n*-octanoyl and total ghrelin as well as the minor population of *n*-decanoyl ghrelin in murine stomach throughout the suckling and weaning periods during which energy metabolism is dramatically altered. Furthermore, we investigated the effect of dietary medium-chain triacylglycerides (MCTs) on the stomach levels of *n*-octanoyl and total ghrelin.

Materials and Methods

Animals

Male C57BL/6J mice and male Wistar rats were used in this experiment. They were maintained under controlled temperature (21–23 C)

First Published Online March 3, 2005

Abbreviations: acyl-modified ghrelin, Ghrelin peptide whose Ser^3 residue is modified by an acyl group such as C8:0, C10:0, or C10:1; C-RIA, RIA to the C-terminus of ghrelin (residues 13–28); *des*-acyl or *des*-octanoyl ghrelin, a ghrelin peptide without acyl modification; GHS, GH secretagogue; GHS-R, GH secretagogue receptor, including two subtypes (GHS-R1a and GHS-R1b); ghrelin-LI, ghrelin-like immunoreactivity; *n*-decanoyl ghrelin, a minor form of ghrelin whose Ser^3 residue is modified by an *n*-decanoyl group (C10:0, a 10-carbon chain lacking a double bond); *n*-decenoyl ghrelin, a second minor form of ghrelin whose Ser^3 residue is modified by an *n*-decenoyl group (C10:1, a 10-carbon chain containing one double bond); *n*-octanoyl ghrelin, the primary form of biologically active ghrelin in humans and rodents, containing a third amino acid residue (Ser^3) modified with an *n*-octanoyl group (C8:0, an eight-carbon chain containing no double bonds) that acts via GHS-R1a; N-RIA, RIA to the N-terminus of *n*-octanoyl ghrelin (residues 1–11); MCFA, medium-chain fatty acid; MCT, medium-chain triglyceride; NW, normal weaning; PW, premature weaning; RP, reverse phase; TFA, trifluoroacetic acid; total ghrelin, a general term comprising all ghrelin peptides with an intact C-terminus (residues 13–28), including *des*-acyl and all acylated forms of ghrelin.

Endocrinology is published monthly by The Endocrine Society (http://www.endo-society.org), the foremost professional society serving the endocrine community.

and light conditions (lights on, 0700–1900 h) with *ad libitum* access to standard laboratory chow (CE-2, CLEA Co. Ltd., Osaka, Japan) and water. All mice were killed by decapitation, and all rats were killed by exsanguination under anesthesia with an ip injection (30 mg/kg body weight) of sodium pentobarbital (Nembutal injection, Dainippon Pharmaceutical Co., Ltd., Osaka, Japan). All experiments were conducted in accordance with the Kurume University Guide for the Care and Use of Experimental Animals.

RIA for ghrelin

RIAs specific for ghrelin were performed as previously described (6). In brief, two polyclonal antibodies were raised in rabbits against the N terminal (Gly^1-Lys^{11} with *O-n*-octanoylation at Ser^3) or C-terminal (Gln^{13}-Arg^{28}) fragments of rat ghrelin. Both antisera exhibited complete cross-reactivity with human, mouse, and rat ghrelins. The antirat ghrelin-(1–11) antiserum, which specifically recognized the Ser^3 *n*-octanoylated form of ghrelin, does not recognize des-acyl ghrelin, but cross-reacts faintly with other acyl-modified ghrelins. Antirat ghrelin-(13–28) antiserum equally recognizes both des-acyl and all acylated forms of ghrelin with intact C-terminal peptide sequences. In the following sections, the RIA system using the antiserum against the N-terminal fragment of rat ghrelin-(1–11) is termed N-RIA, whereas that specific for the C-terminus [ghrelin-(13–28)] is termed C-RIA. Ghrelin-like immunoreactivity (ghrelin-LI) measured by N-RIA is termed ghrelin N-LI or *n*-octanoyl ghrelin-LI, and ghrelin-LI measured by C-RIA, which reflects the amount of ghrelin peptides with intact C-termini (regardless of the acyl-modification of Ser^3) is termed total ghrelin or ghrelin C-LI.

Preparation of stomach samples for ghrelin assay

Male C57BL/6J mice (birth to 12 wk of age) were maintained under controlled temperature (21–23 C) and light conditions (lights on, 0700–1900 h) with *ad libitum* access to a nursing mother, chow, and water. Stomachs collected from mice were washed twice in PBS (pH 7.4). After measuring the wet weights of each sample, the whole stomach tissue was boiled for 5 min in a 10-fold volume of water to inactivate intrinsic proteases. After cooling on ice, boiled samples were adjusted to 1 M acetic acid-20 mM HCl. Peptides were extracted after homogenization with a Polytron mixer (PT 6100, Kinematica AG, Littan-Luzern, Switzerland). Extract supernatants, isolated after a 15-min centrifugation at 15,000 rpm (12,000 × g), were lyophilized and stored at −80 C. The lyophilized samples were dissolved in RIA buffer before ghrelin RIA.

Preparation of plasma samples for ghrelin assay

Plasma samples from rats were prepared as previously described (1, 6). In brief, truncal blood samples obtained by heart puncture were immediately transferred to chilled polypropylene tubes containing EDTA-2Na (1 mg/ml) and aprotinin (1000 kallikrein inactivator units/ml) and centrifuged at 4 C. Immediately after the plasma was separated, HCl was added to the sample to a final concentration of 0.1 N and then diluted with an equal volume of saline. The sample was loaded onto a Sep-Pak C_{18} cartridge (Waters Corp., Milford, MA) preequilibrated with 0.1% trifluoroacetic acid (TFA) and 0.9% NaCl. The cartridge was washed with 0.9% NaCl and 5% acetonitrile (CH_3CN)/0.1% TFA, then eluted with 60% CH_3CN/0.1% TFA. The eluate was lyophilized and stored at −80 C. Lyophilized samples were dissolved in RIA buffer before ghrelin RIA.

Analysis of molecular forms of acyl-modified ghrelin in murine stomach

To investigate changes in the pattern of ghrelin's acyl modification and the levels of *des*-acyl or acyl-modified ghrelins around the time of initiation of weaning, the molecular properties of stomach ghrelin were analyzed by C_{18} reverse phase (RP) HPLC (3.9 × 150 mm; Symmetry 300, Waters Corp.). Stomach peptides were extracted from 3- or 4-wk-old male mice under normal weaning (NW) conditions or from prematurely weaned (PW) 3-wk-old male mice. Stomach peptides were also extracted from 3-wk-old male rats under NW or PW conditions. PW was performed in manner described previously by Hahn *et al.* (21). In brief, eight pups, regardless of sex, were retained from a litter of Wistar rats or C57BL/6J mice on d 2 after birth, weaned to standard laboratory chaw on d 18, and killed on d 21. The stomach or plasma samples from male-only litters were collected and subjected to peptide extraction. Standard laboratory chow (CE-2) derives its caloric content as follows: carbohydrate, 50.3%; protein, 25.4%; and fat, 4.4%. Peptide extracts from stomachs were subjected to RP-HPLC using a linear gradient of 10–60% CH_3CN/0.1% TFA at a flow rate of 1.0 ml/min. Five hundred-microliter fractions were collected. The ghrelin peptide content in each fraction was measured by ghrelin C-RIA. The retention times obtained for the extracted ghrelin molecules were compared with those of synthetic *des*-acyl, *n*-octanoyl, and *n*-decanoyl ghrelin.

Concentrations of n-octanoyl and total ghrelin in murine stomach after glyceryl trioctanoate ingestion

Three-week-old male C57BL/6J mice were maintained under controlled temperature (21–23 C) and light (lights on, 0700–1900 h) conditions with *ad libitum* access to food, water, and their nursing mothers. Glyceryl trioctanoate (Wako Pure Chemical, Osaka, Japan), a MCT rich in rodent milk lipids, was mixed into standard laboratory chow at a concentration of 5% (wt/wt). After 1 wk, whole stomach samples from MCT-fed and control (4-wk-old) mice were collected and assayed for ghrelin N- or C-RIAs as described above.

Statistical analysis

Data are presented as the mean ± SD. Statistical significance was determined by one-way ANOVA, followed by a *post hoc* test (Scheffé's F test). $P < 0.05$ was considered statistically significant.

Results

Concentration of ghrelin-like immunoreactivity in murine stomachs

To elucidate the regulation of ghrelin acyl modification during the developmental stages after birth, the levels of *n*-octanoyl and total ghrelin immunoreactivity in stomachs of mice from birth to 12 wk of age were measured using ghrelin N- and C-RIAs. The level of *n*-octanoyl ghrelin-LI in the stomach increased from birth to 3 wk of age and then fell significantly between 3 and 4 wk after birth (Fig. 1A). After mice reached 4 wk of age, the level of stomach *n*-octanoyl ghrelin remained unchanged. The amount of total ghrelin-LI also increased from birth to 3 wk of age and subsequently remained unchanged from 3–12 wk of age. No significant change in total ghrelin-LI was noted between 3 and 4 wk of age. The ratio of *n*-octanoyl ghrelin-LI to total ghrelin-LI (N/C-ratio) in stomachs of mice increased throughout the suckling period (from 1–3 wk of age). Thereafter, the N/C ratio fell sharply between 3 and 4 wk of age in proportion to the decline in the amount of *n*-octanoyl ghrelin-LI. After 4 wk of age, no significant change in the N/C ratio was detected in stomachs of mice until 12 wk of age. Patterns similar to those described above were observed in data from two subsequent experiments using the same protocol.

Molecular forms of ghrelin in stomachs from 3- and 4-wk-old mice

To examine whether there was a change in the molecular form of stomach ghrelin peptides before and after the suckling-weaning transition, we fractionated stomach samples from 3- and 4-wk-old mice by RP-HPLC and measured ghrelin levels by C-RIA (Fig. 2). Based on the observed retention times of synthetic ghrelin peptides, peaks a and a′ correspond to *des*-acyl ghrelin, peaks b and b′ correspond to

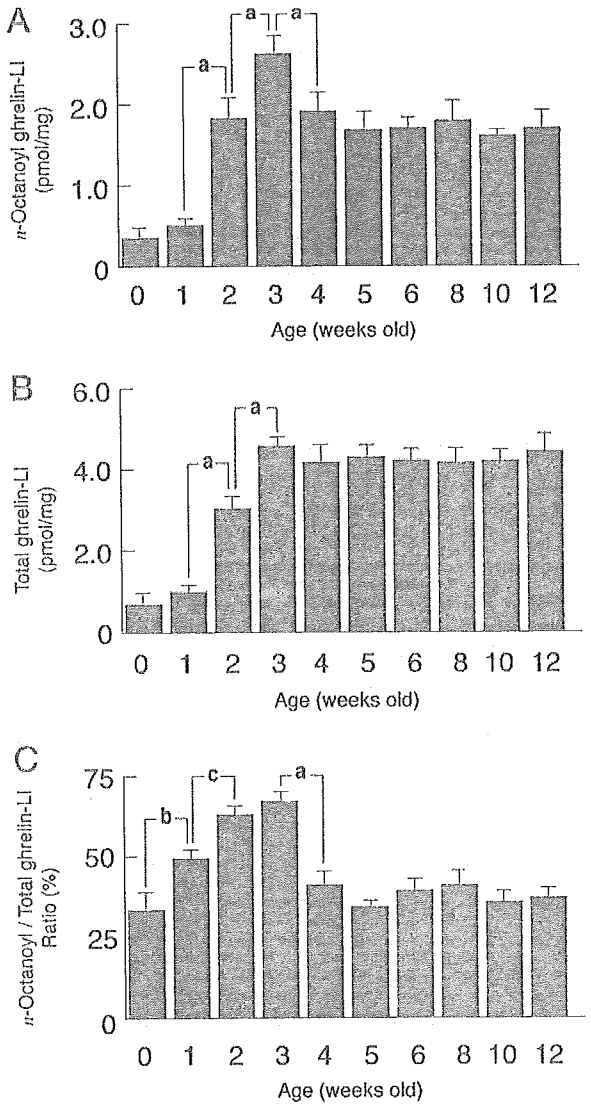

FIG. 1. Amount of ghrelin-LI in the stomachs of mice from birth to 12 wk of age. Each *bar* represents means ± SD (n = 6–12/group). A, *n*-Octanoyl-modified ghrelin-LI concentrations measured by ghrelin N-RIA. B, Total ghrelin-LI (des-acyl and acyl-modified forms of ghrelin with intact C terminus) concentration measured by ghrelin C-RIA. C, The ratio of *n*-octanoyl/total ghrelin-LI in murine stomach (N/C ratio). Statistical significance is indicated by *superscript letters*. a, $P < 0.001$; b, $P < 0.05$; c, $P < 0.01$ (*vs.* the indicated values).

n-octanoyl ghrelin modified by an *n*-octanoyl (C8:0) group, and peaks c and c′ corresponded to *n*-decanoyl ghrelin modified by an *n*-decanoyl (C10:0) group. Compared with 3-wk-old mice, a decrease in the amount of *n*-decanoyl ghrelin (Fig. 2, *upper* panel; peak c: retention time, 24–25 min) was observed in 4-wk-old mice. The level of *n*-octanoyl ghrelin (peak b′: retention time, 20.5–21.5 min) was also decreased in 4-wk-old mice compared with 3-wk-old mice (peak b). In contrast, the level of *des*-acyl ghrelin (peak a′: retention time, 10.5–11.5) in 4-wk-old mouse stomachs was higher than that in 3-wk-old mice (peak a). There was an unidentified peak between peaks b (b′) and c (c′), and there were at least two peaks between peaks a (a′) and b (b′).

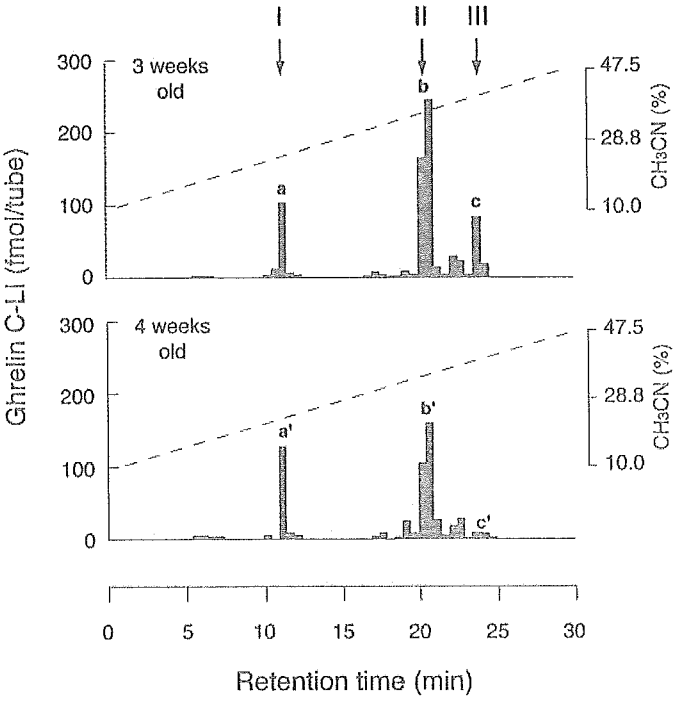

FIG. 2. Molecular forms of ghrelin in the stomachs of 3- and 4-wk-old mice. Peptide extracts from fresh stomachs were fractionated by C_{18} RP-HPLC, and the ghrelin immunoreactivity of the extract was measured by C-RIA (ghrelin C-LI). An assay tube contained equivalent quantities of peptide extract derived from 0.2 mg stomach tissue. ▩, Ghrelin C-LI in each HPLC fraction. *Arrows* indicate the elution of synthetic *des*-acyl ghrelin (I), *n*-octanoyl ghrelin (II), and *n*-decanoyl ghrelin (III). Based on the retention times of synthetic ghrelin peptides, peaks a and a′ correspond to *des*-acyl ghrelin, peaks b and b′ corresponded to *n*-octanoyl ghrelin, and peaks c and c′ correspond to *n*-decanoyl ghrelin.

Concentrations of des-acyl, n-octanoyl, and n-decanoyl ghrelin in stomachs of growing mice

To confirm in detail the change in stomach concentrations of *des*-acyl and acyl-modified ghrelins between 3- and 4-wk-old mice and to check the influence of diet composition on the stomach concentrations of ghrelin molecules, the levels of *des*-acyl and acyl-modified ghrelins in 3- and 4-wk-old mice under NW and PW conditions (n = 8 each) were measured and statistically analyzed after HPLC fractionation (Fig. 3). Compared with 3-wk-old mice, the amounts of *n*-octanoyl and *n*-decanoyl ghrelin were significantly decreased in 4-wk-old mice (Fig. 3, B and C). No significant change was observed in the stomach concentration of des-acyl ghrelin between 3- and 4-wk-old mice (Fig. 3A). Compared with NW mice, the amounts of *n*-octanoyl and *n*-decanoyl ghrelin in stomachs of PW mice were significantly decreased (Fig. 3, B and C). No significant change was observed in the stomach concentration of des-acyl ghrelin between NW and PW mice (Fig. 3A). The average body weights of the PW mice just before (d 18) and after (d 21) the treatment were 7.6 ± 0.6 and 9.1 ± 0.5 g (n = 8), respectively. The average body weights of NW mice on d 18 and 21 were 7.6 ± 0.6 and 8.2 ± 0.3 g (n = 8), respectively. A significant increase in body weight on d 21 was observed in PW mice compared with NW mice ($P < 0.01$).

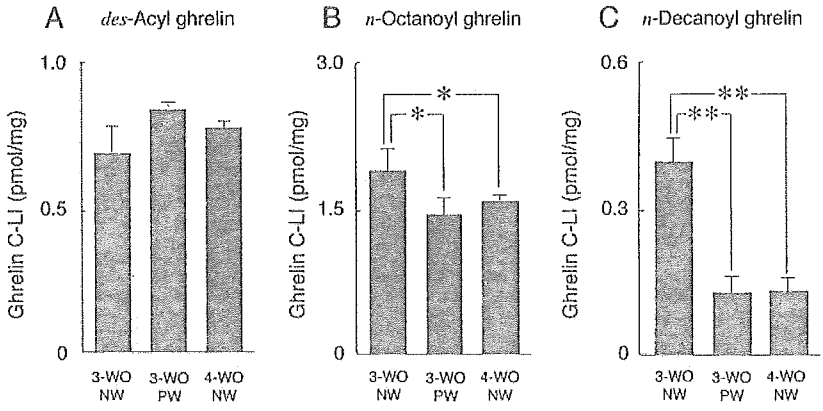

FIG. 3. Concentrations of *des*-acyl, *n*-octanoyl, and *n*-decanoyl ghrelin peptides in stomachs of 3-wk-old NW and PW mice and 4-wk-old NW mice. The stomach amounts of *des*-acyl, *n*-octanoyl, and *n*-decanoyl ghrelin-LI were measured by ghrelin C-RIA after HPLC fractionation. A, *Des*-acyl ghrelin; B, *n*-octanoyl ghrelin; C, *n*-decanoyl ghrelin concentrations in murine stomach. Each *bar* represents mean ± SD of samples obtained by HPLC fractionation (n = 8). *, $P < 0.05$; **, $P < 0.01$ (*vs.* the indicated values).

Plasma and stomach concentrations of n-octanoyl and total ghrelin from normally weaned and prematurely weaned rats

To clarify whether the proportion of *n*-octanoyl ghrelin in the circulation is also influenced by diet composition, plasma concentrations of *n*-octanoyl and total ghrelin from 3-wk-old NW and PW rats were measured by ghrelin N- and C-RIAs. Stomach concentrations of *n*-octanoyl and total ghrelin were measured in the same rats. As shown in Fig. 4A, the plasma *n*-octanoyl ghrelin levels were significantly lower in PW rats compared with NW rats. The plasma total ghrelin concentration was increased slightly, but not significantly, in PW compared with NW rats (Fig. 4B). The amount of *n*-octanoyl ghrelin in the stomachs of PW rats was lower than that in NW rats (Fig. 4D). However, the level of total ghrelin in the stomachs of PW rats was significantly higher than that in NW rats (Fig. 4E). Consequently, the proportions of *n*-octanoyl ghrelin to total ghrelin in both the circulation and the stomach were decreased in prematurely weaned rats (Fig. 4, C and F). The average body weights of the PW rats just before (d 18) and after (d 21) the treatment were 41.3 ± 2.8 and 54.9 ± 3.3 g (n = 8), respectively. The average body weights of the NW rats on d 18 and 21 were 41.7 ± 2.8 and 55.6 ± 2.6 g (n = 8), respectively.

Stomach concentrations of n-octanoyl and total ghrelin after glyceryl trioctanoate ingestion

To examine whether the ingestion of MCTs, which are found in high levels in milk lipids, influences the acyl mod-

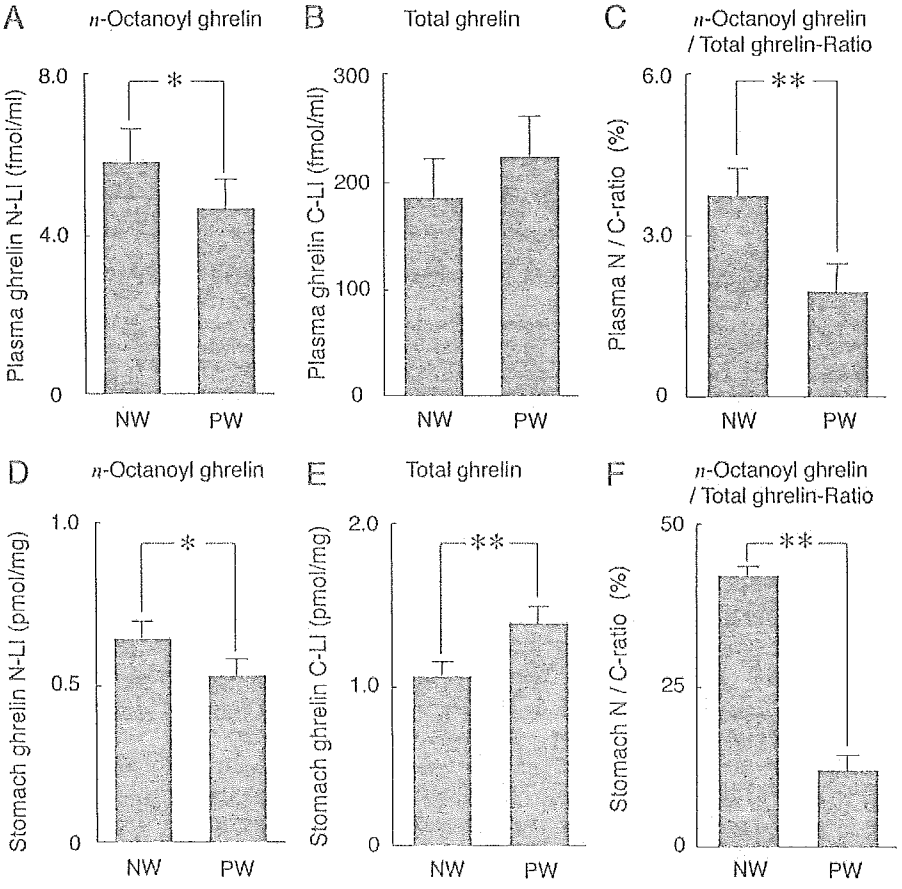

FIG. 4. Concentrations of plasma and stomach ghrelin in NW and PW rats. A, Concentrations of plasma *n*-octanoyl ghrelin measured by ghrelin N-RIA (ghrelin N-LI). B, Plasma total ghrelin concentrations measured by ghrelin C-RIA (ghrelin C-LI). C, The ratio of *n*-octanoyl ghrelin-LI to total ghrelin-LI (N/C-ratio) in plasma calculated from plasma ghrelin N- and C-LI. D, Concentrations of stomach *n*-octanoyl ghrelin measured by ghrelin N-RIA (ghrelin N-LI). E, Concentrations of stomach total ghrelin measured by ghrelin C-RIA (ghrelin C-LI). F, The ratio of *n*-octanoyl ghrelin-LI to total ghrelin-LI (N/C-ratio) in stomach calculated from stomach ghrelin N- and C-LI. Data represent the mean ± SD of samples (n = 8). *, $P < 0.05$; **, $P < 0.01$ (*vs.* the indicated values).

ification of ghrelin, the stomach concentrations of *n*-octanoyl and total ghrelin were measured by N- and C-RIAs after feeding chow mixed with 5% glyceryl trioctanoate (C8:0-MCT) to 3-wk-old mice for 1 wk (from 3–4 wk after birth; n = 8). Compared with control mice fed a standard laboratory chow, a significant increase in the stomach concentration of *n*-octanoyl ghrelin was observed (Fig. 5). The proportion of *n*-octanoyl ghrelin to total ghrelin was also increased, because there was a slight, but not significant, decline in the level of total ghrelin in the stomachs of these mice. There was no significant difference between the body weights of C8:0-MCT-fed (19.1 ± 2.4 g) and control (standard CE-2 laboratory chow-fed; 19.6 ± 2.0 g) mice on the day of ghrelin RIA.

Discussion

In this study we demonstrated that the level of *n*-octanoyl ghrelin in mouse stomach increased gradually throughout the suckling period and then decreased sharply after weaning. In contrast, the total ghrelin concentration in mouse stomach, measured by ghrelin C-RIA, did not show a significant change during the suckling-weaning transition. Consequently, the proportion of *n*-octanoyl ghrelin to total ghrelin exhibited a significant decrease after weaning.

To date, four reports have been published about developmental changes in stomach ghrelin production (14, 22–24). It has been difficult, however, to compare these previous findings with our current data, because the methods used to calculate and analyze stomach ghrelin concentrations are different from those we employed, and none of these previous reports recorded the change in the ratio of acyl-modified ghrelin to total ghrelin in the stomach.

Because it was difficult to obtain large plasma samples from mice, we used Wistar rats to measure changes in the level of circulating *n*-octanoyl ghrelin during the suckling-weaning transition. Stomach *n*-octanoyl ghrelin levels were found to decline at a similar rate in PW rats and PW mice. We observed a low ratio of plasma *n*-octanoyl ghrelin to total ghrelin in 3-wk-old PW rats compared with NW rats of the same age. Our findings largely corroborate those of Raff *et al.* (24), who reported recently that the plasma concentration of active, *n*-octanoyl-modified ghrelin after the weaning period, at 35 d of age, was significantly lower than that seen at 7 d, during the suckling period (7 d of age) in rats. However, in our study we also observed a slight increase in the amount of plasma total ghrelin together with a significant increase in the stomach total ghrelin concentration in PW rats. Because the circulating ghrelin level is determined by a delicate balance among the secretion rate (mainly from stomach), the degradation rate (*des*-acylation by plasma esterase and/or degradation of peptide by plasma proteases), and the clearance rate (capture by ghrelin receptor or urinary clearance) of this acyl-modified peptide, it is unlikely that the concentration of *n*-octanoyl or total ghrelin in the circulation simply reflects the stomach concentration of each form of ghrelin under all metabolic conditions.

In addition to its functions within the endocrine system, ghrelin exerts biological effects using autocrine, paracrine (25, 26), and/or neuroendocrine (27–30) pathways. Therefore, it is possible that the change in the level of *n*-octanoyl ghrelin in murine stomach during the suckling-weaning transition could act through pathways independent of circulating ghrelin.

Despite a significant decrease in the proportion of stomach *n*-octanoyl ghrelin, 21-d-old PW mice exhibited a significantly larger increase in body weight compared with NW mice. This result is counterintuitive in light of ghrelin's close association with adiposity (8, 31). However, the amount of stomach *n*-octanoylated ghrelin measured in the PW mice may not truly reflect the physiological ghrelin balance in these animals. First, the rapid development that occurs after birth and the concomitant negative energy balance may accelerate the secretion of *n*-octanoyl ghrelin from the stomach to the circulation, thus aberrantly lowering its stomach levels even though the production of stomach ghrelin (including both acylated and nonacylated forms) remains high. Furthermore, plasma esterases quickly deacylate ghrelin peptides upon their entry into the circulation (32), thus lowering the plasma concentration of acylated ghrelin. In these ways, rapid turnover of acylated ghrelin could mask an increase in its production, giving rise to the unexpected correlation of decreased stomach acylated ghrelin and increased body weight in PW mice. This hypothesis is partly supported by our data for stomach and plasma concentrations of *n*-octanoyl and total ghrelin in PW rats, although there was no significant difference between the average body weights of the PW and NW rats a short time (3 d) after treatment.

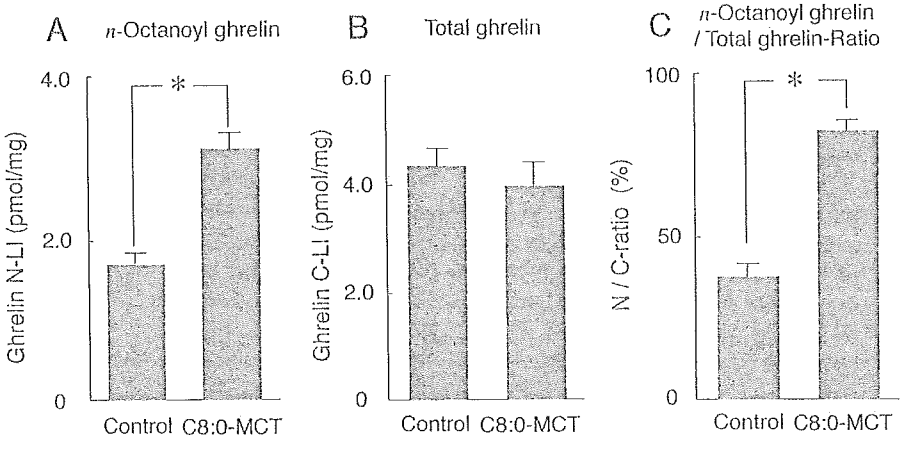

FIG. 5. Stomach concentrations of *n*-octanoyl and total ghrelin in 4-wk-old mice that ingested glyceryl trioctanoate (C8:0-MCT) for 1 wk (from 3–4 wk of age). A, *n*-Octanoyl ghrelin concentrations measured by ghrelin N-RIA (n = 8). B, Total ghrelin concentrations measured by ghrelin C-RIA (n = 8). C, The ratio of *n*-octanoyl ghrelin-LI to total ghrelin-LI (N/C-ratio) calculated from the ghrelin N- and C-LI (n = 8). *, $P < 0.01$ (*vs.* the indicated values).

Throughout the suckling period, over 60% of a rodent's energy is derived from milk lipids, primarily triglycerides (33, 34). After weaning, there is a progressive rise in the proportion of energy supplied by carbohydrates (35). During the suckling-weaning transition, energy metabolism as well as the secretion and production of ghrelin are dramatically altered under the influence of various components of the diet. Lee *et al.* (14) demonstrated that in rats, the rate of ghrelin's production, as indicated by the stomach ghrelin mRNA level, as well as its secretion, as indicated by the plasma ghrelin level, are both increased under low protein and high carbohydrate diets. In contrast, the rates of production and secretion of ghrelin were both decreased by high fat diets. These diet-related changes in ghrelin production and secretion rates might influence the proportion of acyl-modified ghrelin in murine stomach.

During the suckling-weaning transition, the production and secretion rates of hormones that influence energy metabolism are also dramatically changed in conjunction with the change in energy source. The concentration of serum T_4 gradually rises after birth to maximal levels just before the initiation of weaning and remains high until the fourth week of life (36). The concentration of plasma glucagon declines (37, 38), and plasma insulin (39) and corticosterone levels (40) rise after the initiation of weaning. These changes in hormone secretion together with the secretion of ghrelin, in turn, influence the activity of energy-metabolizing enzymes in liver and peripheral tissues (35).

Our finding that the stomach concentration of *n*-octanoyl ghrelin rises significantly after the ingestion of glyceryl trioctanoate is interesting, because there is a high proportion of MCTs and medium-chain fatty acids (MCFAs) in the milk lipids of rodents (41, 42). A significant decrease in the stomach levels of *n*-octanoyl and *n*-decanoyl ghrelin after the initiation of weaning (~4 wk of age) implies that MCTs and MCFAs in milk lipids may be sources for acyl groups that can attach to the Ser^3 residue of ghrelin during the suckling period.

Orally ingested MCFAs and those hydrolyzed from ingested MCTs are directly absorbed from gastric and intestinal mucosa (43), where ghrelin-producing cells are found. Therefore, it appears possible that the orally ingested MCFAs and those hydrolyzed from ingested MCTs can diffuse into the ghrelin-producing cells and serve as a nutrient signal by interfering with the acyl modification of ghrelin. It is also possible that endogenously synthesized MCFAs and their derivatives that are produced upon lipid metabolism are transferred to the ghrelin-producing cells and used in the acyl modification of ghrelin.

Additional study is required to elucidate in detail the relationship between the acyl modification of ghrelin and energy metabolism. It also remains to be determined whether ingested MCTs directly modulate the Ser^3 residue of ghrelin peptide or indirectly stimulate the acyl modification of ghrelin through the induction of an acyl-modifying enzyme. Our new findings described here provide important clues to enhance our understanding of the regulation of ghrelin acyl modification during the development of the murine stomach.

Acknowledgments

We thank Prof. H. Nawata and Dr. T. Yanase for reading and reviewing the draft of our manuscript, K. Shirouzu and Y. Yamashita for their technical assistance, and Drs. H. Hosoda and H. Kaiya for providing us antibodies and tracers for ghrelin RIA.

Received May 21, 2004. Accepted February 18, 2005.

Address all correspondence and requests for reprints to: Dr. Masayasu Kojima, Molecular Genetics, Institute of Life Science, Kurume University, Kurume, Fukuoka 839-0861, Japan. E-mail: mkojima@lsi.kurume-u.ac.jp.

This work was supported by the Program for Promotion of Basic Research Activities for Innovative Biosciences (PROBRAIN); a Grant-in-Aid for Scientific Research (B) from the Ministry of Education, Culture, Sports, Science, and Technology of Japan; the Uehara Foundation; the Yamanouchi Foundation for Research on Metabolic Disorders; the Takeda Science Foundation; the Brain Science Foundation; the Naito Foundation; the Japan Foundation for Applied Enzymology; a grant-in-aid from the Tokyo Biochemical Research and the Mitsubishi Foundation (to M.K.); and MEXT Open Research Project (2004). This work was also supported by a grant-in-aid for the Promotion of Fundamental Studies in Health Science from the Organization for Pharmaceutical Safety and Research of Japan (to K.K.).

References

1. Kojima M, Hosoda H, Date Y, Nakazato M, Matsuo H, Kangawa K 1999 Ghrelin is a growth-hormone-releasing acylated peptide from stomach. Nature 402:656–660
2. Kojima M, Hosoda H, Matsuo H, Kangawa K 2001 Ghrelin: discovery of the natural endogenous ligand for the growth hormone secretagogue receptor. Trends Endocrinol Metab 12:118–122
3. Bowers CY, Momany F, Reynolds GA, Chang D, Hong A, Chang K 1980 Structure-activity relationships of a synthetic pentapeptide that specifically releases growth hormone *in vitro*. Endocrinology 106:663–667
4. Patchett AA, Nargund RP, Tata JR, Chen MH, Barakat KJ, Johnston DB, Cheng K, Chan WW, Butler B, Hickey G 1995 Design and biological activities of L-163,191 (MK-0677): a potent, orally active growth hormone secretagogue. Proc Natl Acad Sci USA 92:7001–7005
5. Smith RG, Van der Ploeg LH, Howard AD, Feighner SD, Cheng K, Hickey GJ, Wyvratt Jr MJ, Fisher MH, Nargund RP, Patchett AA 1997 Peptidomimetic regulation of growth hormone secretion. Endocr Rev 18:621–645
6. Hosoda H, Kojima M, Matsuo H, Kangawa K 2000 Ghrelin and des-acyl ghrelin: two major forms of rat ghrelin peptide in gastrointestinal tissue. Biochem Biophys Res Commun 279:909–913
7. Nakazato M, Murakami N, Date Y, Kojima M, Matsuo H, Kangawa K, Matsukura S 2001 A role for ghrelin in the central regulation of feeding. Nature 409:194–198
8. Tschop M, Smiley DL, Heiman ML 2000 Ghrelin induces adiposity in rodents. Nature 407:908–913
9. Matsumoto M, Hosoda H, Kitajima Y, Morozumi N, Minamitake Y, Hosoda H, Kojima M, Matsuo H, Kangawa K 2001 Structure-activity relationship of ghrelin: pharmacological study of ghrelin peptides. Biochem Biophys Res Commun 287:142–146
10. Hosoda H, Kojima M, Matsuo H, Kangawa K 2000 Purification and characterization of rat des-Gln^{14}-ghrelin, a second endogenous ligand for the growth hormone secretagogue receptor. J Biol Chem 275:21995–22000
11. Hosoda H, Kojima M, Mizushima T, Shimizu S, Kangawa K 2003 Structural divergence of human ghrelin. Identification of multiple ghrelin-derived molecules produced by post-translational processing. J Biol Chem 278:64–70
12. Kaiya H, Kojima M, Hosoda H, Koda A, Yamamoto K, Kitajima Y, Matsumoto M, Minamitake Y, Kikiyama S, Kangawa K 2001 Bullfrog ghrelin is modified by *n*-octanoic acid at its third threonine residue. J Biol Chem 276:40441–40448
13. Kaiya H, Van Der Geyten S, Kojima M, Hosoda H, Kitajima Y, Matsumoto M, Geelissen S, Darras VM, Kangawa K 2002 Chicken ghrelin: purification, cDNA cloning, and biological activity. Endocrinology 143:3454–3463
14. Lee HM, Wang G, Englander EW, Kojima M, Greeley Jr GH 2002 Ghrelin, a new gastrointestinal endocrine peptide that stimulates insulin secretion: enteric distribution, ontogeny, influence of endocrine, and dietary manipulations. Endocrinology 143:185–190
15. Shiiya T, Nakazato M, Mizuta M, Date Y, Mondal MS, Tanaka M, Nozoe S, Hosoda H, Kangawa K, Masukura S 2002 Plasma ghrelin levels in lean and obese humans and the effect of glucose on ghrelin secretion. J Clin Endocrinol Metab 87:240–244
16. Cummings DE, Weigle DS, Frayo RS, Breen PA, Ma MK, Dellinger EP, Purnell JQ 2002 Plasma ghrelin levels after diet-induced weight loss or gastric bypass surgery. N Engl J Med 346:1623–1630
17. Riis AL, Hansen TK, Moller N, Weeke J, Jorgensen JO 2003 Hyperthyroidism

is associated with suppressed circulating ghrelin levels. J Clin Endocrinol Metab 88:853–857
18. Sugino T, Yamaura J, Yamagishi M, Kurose Y, Kojima M, Kangawa K, Hasegawa Y, Terashima Y 2003 Involvement of cholinergic neurons in the regulation of the ghrelin secretory response to feeding in sheep. Biochem Biophys Res Commun 304:308–312
19. Ariyasu H, Takaya K, Hosoda H, Iwakura H, Ebihara K, Mori K, Ogawa Y, Hosoda K, Akamizu T, Kojima M, Kangawa K, Nakao K 2002 Delayed short-term secretory regulation of ghrelin in obese animals: evidenced by a specific RIA for the active form of ghrelin. Endocrinology 143:3341–3350
20. Marzullo P, Verti B, Savia G, Walker GE, Guzzaloni G, Tagliaferri M, Di Blasio A, Liuzzi A 2004 The relationship between active ghrelin levels and human obesity involves alterations in resting energy expenditure. J Clin Endocrinol Metab 89:936–939
21. Hahn P, Kirby L 1973 Immediate and late effects of premature weaning and of feeding a high fat or high carbohydrate diet to weanling rats. J Nutr 103:690–696
22. Hayashida T, Nakahara K, Mondal MS, Date Y, Nakazato M, Kojima M, Kangawa K, Murakami N 2002 Ghrelin in neonatal rats: distribution in stomach and its possible role. J Endocrinol 173:239–245
23. Sakata I, Tanaka T, Matsubara M, Yamazaki M, Tani S, Hayashi Y, Kangawa K, Sakai T 2002 Postnatal changes in ghrelin mRNA expression and in ghrelin-producing cells in the rat stomach. J Endocrinol 174:463–471
24. Raff H 2003 Total and active ghrelin in developing rats during hypoxia. Endocrine 21:159–161
25. Kamegai J, Tamura H, Shimizu T, Ishii S, Tatsuguchi A, Sugihara H, Oikawa S, Kineman RD 2004 The role of pituitary ghrelin in growth hormone (GH) secretion: GH-releasing hormone-dependent regulation of pituitary ghrelin gene expression and peptide content. Endocrinology 145:3731–3738
26. Jeffery PL, Herington AC, Chopin LK 2003 The potential autocrine/paracrine roles of ghrelin and its receptor in hormone-dependent cancer. Cytokine Growth Factor Rev 14:113–122
27. Date Y, Murakami N, Toshinai K, Matsukura S, Niijima A, Matsuo H, Kangawa K, Natazato M 2002 The role of the gastric afferent vagal nerve in ghrelin-induced feeding and growth hormone secretion in rats. Gastroenterology 123:1120–1128
28. Sibilia V, Rindi G, Pagani F, Rapetti D, Locatelli V, Torsello A, Campanini N, Deghenghi R, Netti C 2003 Ghrelin protects against ethanol-induced gastric ulcers in rats: studies on the mechanisms of action. Endocrinology 144:353–359
29. Fujino K, Inui A, Asakawa A, Kihara N, Fujimura M, Fujimiya M 2003 Ghrelin induces fasted motor activity of the gastrointestinal tract in conscious fed rats. J Physiol 550:227–240
30. Sakata I, Yamazaki M, Inoue K, Hayashi Y, Kangawa K, Sakai T 2003 Growth hormone secretagogue receptor expression in the cells of the stomach-projected afferent nerve in the rat nodose ganglion. Neurosci Lett 342:183–186
31. Wren AM, Small CJ, Abbott CR, Dhillo WS, Seal LJ, Cohen MA, Batterham RL, Taheri S, Stanley SA, Ghatei MA, Bloom SR 2001 Ghrelin causes hyperphagia and obesity in rats. Diabetes 50:2540–2547
32. De Vriese C, Gregoire F, Lema-Kisoka R, Waelbroeck M, Robberecht P, Delporte C 2004 Ghrelin degradation by serum and tissue homogenates: identification of the cleavage sites. Endocrinology 145:4997–5005
33. Dymsza HA, Czajka DM, Miller SA 1964 Influence of artificial diet on weight gain and body composition of the neonatal rat. J Nutr 84:100–106
34. Chalk PA, Bailey E 1979 Changes in the yield, and carbohydrate, lipid and protein content of milk during lactation in the rat. J Dev Physiol 1:61–79
35. Angel JF, Back DW 1985 Weaning and metabolic regulation in the rat. Can J Physiol Pharmacol 63:538–545
36. Dussault JH, Labrie F 1975 Development of the hypothalamic-pituitary-thyroid axis in the neonatal rat. Endocrinology 97:1321–1324
37. Beaudry MA, Chiasson JL, Exton JH 1977 Gluconeogenesis in the suckling rat. Am J Physiol 233:E175–E180
38. Hahn P, Girard J, Assan R, Frohlich J, Kervran A 1977 Control of blood cholesterol levels in suckling and weanling rats. J Nutr 107:2062–2066
39. Blazquez E, Montoya E, Lopez Quijada C 1970 Relationship between insulin concentrations in plasma and pancreas of foetal and weanling rats. J Endocrinol 48:553–561
40. Henning SJ 1978 Plasma concentrations of total and free corticosterone during development in the rat. Am J Physiol 235:E451–E456
41. Smith S, Watts R, Dils R 1968 Quantitative gas-liquid chromatographic analysis of rodent milk triglycerides. J Lipid Res 9:52–57
42. Bitman J, Wood DL, Liao TH, Fink CS, Hamosh P, Hamosh M 1985 Gastric lipolysis of milk lipids in suckling rats. Biochim Biophys Acta 834:58–64
43. Greenberger NJ, Skillman TG 1969 Medium-chain triglycerides. N Engl J Med 280:1045–1058

Endocrinology is published monthly by The Endocrine Society (http://www.endo-society.org), the foremost professional society serving the endocrine community.

Available online at www.sciencedirect.com

SCIENCE DIRECT®

Regulatory Peptides 128 (2005) 7–13

REGULATORY PEPTIDES

www.elsevier.com/locate/regpep

Chronic administration of adrenomedullin attenuates the hypertension and increases renal nitric oxide synthase in Dahl salt-sensitive rats

Fumiki Yoshihara[a,*], Shin-ichi Suga[b], Naomi Yasui[b], Takeshi Horio[a], Takeshi Tokudome[b], Toshio Nishikimi[c], Yuhei Kawano[a], Kenji Kangawa[b]

[a]*Division of Hypertension and Nephrology, National Cardiovascular center, 5-7-1 Fujishirodai, Suita, Osaka 565-8565, Japan*
[b]*National Cardiovascular Center Research Institute, 5-7-1 Fujishirodai, Suita, Osaka 565-8565, Japan*
[c]*Department of Hypertension and Cardiorenal Medicine, Dokkyo University School of Medicine, Mibu, Tochigi 321-0293, Japan*

Received 16 June 2004; accepted 10 December 2004
Available online 27 January 2005

Abstract

Adrenomedullin reduces systemic blood pressure and increases urinary sodium excretion partly through the release of nitric oxide. We hypothesized that chronic adrenomedullin infusion ameliorates salt-sensitive hypertension and increases the expression of renal nitric oxide synthase (NOS) in Dahl salt-sensitive (DS) rats, because the reduced renal NOS expression promotes salt sensitivity. DS rats and Dahl salt-resistant (DR) rats were fed a high sodium diet (8.0% NaCl) for 3 weeks. The high sodium diet resulted in an increase in blood pressure and a reduction of urinary sodium excretion in association with increased renal adrenomedullin concentrations and decreased expression of renal neuronal NOS (nNOS) and renal medullary endothelial NOS (eNOS) in DS rats compared with DR rats. Chronic adrenomedullin infusion partly inhibited the increase of blood pressure and proteinuria in association with a restoration of renal nNOS and medullary eNOS expression in DS rats under the high sodium diet. The immunohistochemical analysis revealed that the restored renal nNOS expression induced by chronic adrenomedullin infusion may reflect the restoration of nNOS expression in the macula densa and inner medullary collecting duct. These results suggest that adrenomedullin infusion has beneficial effects on this hypertension probably in part through restored renal NOS expression in DS rats.

Keywords: Adrenomedullin; Kidney; Nitric oxide synthase; Rats; Dahl; Western blot

1. Introduction

Salt sensitivity has been reported to be an independent cardiovascular risk factor in patients with hypertension [1], suggesting that the investigation of renal mechanisms of salt sensitivity is necessary to open up a possible new therapeutic strategy for hypertension. Nitric oxide (NO) was reported to stimulate an adaptive response to increased dietary sodium intake, cause vasodilation, and facilitate natriuresis [2]. The inhibition of nitric oxide synthase (NOS) was found to blunt the pressure–natriuresis relationship in normotensive rats [3], suggesting that an impaired NOS may be one of the factors causing salt-sensitive hypertension [4]. Furthermore, the reduced renal neuronal NOS (nNOS) activity in rats with salt-sensitive hypertension has been reported to promote salt sensitivity [5].

Adrenomedullin is a vasodilatory peptide originally discovered in human pheochromocytoma tissue [6]. Subsequent studies demonstrated that adrenomedullin and its specific binding sites are widely distributed in the cardiovascular system, including the kidney, heart, lungs and blood vessels [6,7]. Adrenomedullin immunoreactivity exists in glomeruli, cortical distal tubules, and medullary collecting duct cells [8]. These results suggest that adrenomedullin may play a role in the regulation of renal function. Indeed, intrarenal infusion of adrenomedullin increased the renal blood flow, glomerular filtration rate, renal sodium excretion [8]. Adrenomedullin also regulates

* Corresponding author. Tel.: +81 6 6833 5012; fax: +81 6 6872 7486.
E-mail address: fyoshi@ri.ncvc.go.jp (F. Yoshihara).

0167-0115/$ - see front matter © 2005 Elsevier B.V. All rights reserved.
doi:10.1016/j.regpep.2004.12.028

the NO production. Recently, adrenomedullin has been reported to induce NO production via the Ca^{2+}/calmodulin-dependent pathway in cultured endothelial cells [9]. These results suggested that adrenomedullin may participate in the regulation of NO production through the stimulation of eNOS and nNOS which are activated by calcium and calmodulin, and renal sodium excretion in rats with salt-sensitive hypertension.

We hypothesized that renal adrenomedullin participates in the regulation of salt sensitivity by modulating renal eNOS and nNOS, and that chronic adrenomedullin infusion ameliorates salt-sensitive hypertension and increases the expression of renal nitric oxide synthase (NOS) in Dahl salt-sensitive (DS) rats.

Thus, the purposes of this study were 1) to investigate whether the renal adrenomedullin level correlates with systemic blood pressure and urinary sodium excretion, 2) to examine whether adrenomedullin supplementation improves the salt-sensitive hypertension and affects the altered renal eNOS and nNOS expression, and 3) to evaluate where nNOS exists in the kidney in DS rats.

2. Materials and methods

2.1. Experimental animals

We used 6-week-old male DS rats and Dahl salt-resistant (DR) rats (Eisai Co. Ltd. Tokyo, Japan) in the present study. This study was performed in accordance with the guidelines of the Animal Care Committee of the National Cardiovascular Center Research Institute.

2.2. Protocol 1

The total experimental period was 4 weeks. The animals (DR rats: n=22, DS rats: n=23) were fed a regular sodium diet (0.5% NaCl) for 1 week followed by a high sodium diet (8.0% NaCl) for 3 weeks during our experimental protocol. The rats were sacrificed and the kidneys were excised for the analyses at the end of the 2nd-, 3rd-, and 4th-week of the study.

2.2.1. Urinary parameters

Twenty-four-hour urinary samples were collected from rats in metabolic cages at the end of the 1st-, 2nd-, 3rd-, and 4th-week of the study for the measurement of urinary volume and sodium excretion level. The urinary sodium level was measured by an auto-analyzer.

2.2.2. Blood pressure measurements

Systolic blood pressure was measured in conscious, restrained rats before the day of the urinary collection in every week by the tail cuff method with automated sphygmomanometers. Rats were placed in individual restrainers and pre-warmed at 37 °C. The average of three readings was recorded.

2.2.3. Measurements of renal tissue adrenomedulln

The rat adrenomedullin levels in the renal cortex and medulla were measured at the end of the 4th-week of the study in DS and DR rats. Radioimmunoassay for rat adrenomedullin was performed as described previously [10].

2.2.4. Western blot analysis

Western blotting for eNOS and nNOS in the renal cortex and medulla (DR rats, n=4; DS rats, n=4) was carried out at the end of the 4th-week of the study [11]. Twenty-microgram kidney tissue preparations were size-fractionated on 4–12% Tris-Glycine gel (Bio-Rad) at 200V for 1.5 h. After electrophoresis, proteins were transferred onto Immobilon-P membrane (Millipore) at 350 mA for 100 min. The membrane was prehybridized in 10 mL of TBST (10 mmol/L Tris hydrochloride, pH 7.5, 100 mmol/L NaCl, 0.1% Tween 20) containing 5% nonfat milk for 2 h and hybridized overnight in the same buffer containing anti-eNOS or anti-nNOS monoclonal antibodies (1:750, Transduction Labs). The membrane was then washed for 30 min with TBST and then incubated with TBST with 5% nonfat milk and goat anti-mouse IgG-horseradish peroxidase (1:1000, Amersham) After the washes, the membrane was developed with a chemiluminating method using ECL reagent (Amersham Inc). The membrane was then subjected to autoluminography for 5–10 min. The autoluminographs were scanned with a laser densitometer to determine the relative optical densities of the bands. The membranes were stained with India ink before prehybridization to confirm an equal amount of protein loading and transfer efficiency among the samples.

2.3. Protocol 2

The experimental period and the feeding protocol were identical to those of protocol 1. Before the 2nd-week, DS rats were randomly divided into 2 groups; the adrenomedullin-treated group and the untreated group. After pentobarbital sodium anesthesia (30 mg/kg, IP), the rats were subcutaneously implanted with an osmotic minipump (Model 2ML4, Alza) filled with recombinant human adrenomedullin dissolved in 0.9% saline in the adrenomedullin-treated group (DS-AM, 400 ng/hr per rat, n=14) and and 0.9% saline in the untreated group (DS-S, n=14). for evaluating the effects of adrenomedullin infusion on systolic blood pressure and urinary sodium excretion under the high sodium diet.

2.3.1. Recombinant human adrenomedullin

Recombinant human adrenomedullin was kindly provided by Shionogi Pharmaceutical, Osaka, Japan. Adrenomedullin with a glycine extension residue at the C-terminus (adrenomedullin-gly) was expressed in *Escherichia coli*. The product was digested with a site-specific protease after denaturation. The resulting adrenomedullin-gly was amidated by a peptidyl-glycine amidating enzyme for conversion to the mature form of adrenomedullin with an amidated C-terminus.

2.3.2. Urinary parameters, blood pressure measurements, and western blot analysis

Twenty-four-hour urinary samples were collected from rats in metabolic cages at the end of each week throughout the study for the measurement of urinary volume and protein excretion. Urinary sodium excretion was measured at the end of 4th-week. Systolic blood pressure was measured before the day of the urine collection. Western blot analysis for eNOS and nNOS in the renal cortex and medulla was performed at the end of protocol 2.

2.3.3. Immunohistochemistry

For immunohistochemical analysis, the kidneys were fixed with Methyl Carnoy. The tissues were embedded in paraffin, and 3-μm-thick sections were cut and mounted on glass slides treated with silica. An indirect immunoperoxidase method was used to identify the nNOS antigen (a mouse IgG to neuronal NOS, Transduction Labs) [12].

2.4. Statistical analysis

All values are presented as mean±SD. Comparisons of 3 or more groups were performed by ANOVA with the Scheffe's post hoc test. Comparisons between 2 groups were performed by the unpaired t test. Differences were considered statistically significant at a level of $p<0.05$. Correlation coefficients were calculated using linear regression analysis.

3. Results

3.1. Protocol 1

Body weight was significantly reduced and left ventricular plus septal weight was significantly increased at the 4th-week in DS rats compared with DR rats (Table 1). Kidney weight was also increased after the 3rd-week in DS rats compared with DR rats (Table 1). Systolic blood pressure and urinary sodium excretion were not significantly different between DS and DR rats at the 2nd-week (Table 1). While systolic blood pressure significantly increased after the 3rd-week, urinary sodium excretion decreased only at the 4th-week in DS rats compared with DR rats (Table 1).

Table 2
Correlations between renal adrenomedullin (AM) concentrations with urinary sodium excretion and systolic blood pressure at the 4th-week in protocol 1

	Cortical AM (fmol/mg)	Medullary AM (fmol/mg)
Urinary Na excretion (mmol/day)	$R=-0.68$, $p<0.01$	$R=-0.60$, $p<0.05$
Systolic Blood Pressure (mmHg)	$R=0.85$, $p<0.0001$	$R=0.86$, $p<0.0001$

The tissue adrenomedullin concentrations in both the renal cortex and medulla were significantly increased at the end of 4th-week in DS rats compared with DR rats (Table 1). The increased renal adrenomedullin levels in the renal cortex and medulla inversely correlated with urinary sodium excretion and positively correlated with systolic blood pressure (Table 2). Western blot analysis revealed that the eNOS expression in the renal medulla and the nNOS expression in both the renal cortex and medulla were significantly lower in DS rats compared with DR rats at the end of the 4th-week (Fig. 1). However, renal cortical eNOS expression was comparable between DS and DR rats (Fig. 1).

3.2. Protocol 2

The chronic adrenomedullin infusion did not affect body and kidney weight in DS rats, however, its infusion significantly reduced the left ventricular and septal weight in DS rats at the end of the 4th-week (Table 3). The chronic adrenomedullin infusion significantly reduced systolic blood pressure and tended to increase urinary sodium excretion at the 4th-week in DS rats under the high sodium diet (Table 3). Chronic adrenomedullin infusion signifi-

Table 1
Number, body weight, heart rate, heart and kidney weights in Dahl rats during feeding on the high sodium diet

	2nd-week		3rd-week		4th-week	
	DR	DS	DR	DS	DR	DS
N	7	8	8	7	7	8
BW (g)	286±16	292±9	309±11	297±14	371±12	342±12**
HR (bpm)	389±24	398±37	396±36	373±10	377±22	399±25
LV+SEP/BW (mg/g)	2.06±0.15	2.19±0.07	2.22±0.16	2.42±0.07	1.97±0.11	2.58±0.13[a]
Kid/BW (mg/g)	3.69±0.26	3.91±0.14	4.09±0.13	4.46±0.20*	3.67±0.13	4.64±0.19[a]
SBP (mmHg)	119±8	126±6	124±9	166±5[a]	125±8	169±7[a]
UNaV (mmol/day)	2.1±1.0	2.4±0.7	1.9±0.6	1.9±0.9	2.7±1.3	1.2±0.3**
Cortical AM (fmol/mg)	0.59±0.10	0.62±0.05	0.56±0.06	0.61±0.09	0.55±0.06	0.74±0.06**
Medullary AM (fmol/mg)	0.31±0.06	0.31±0.05	0.34±0.04	0.31±0.05	0.34±0.02	0.45±0.04**

N indicates number of rats; BW, body weight; HR, heart rate; LV+SEP, left ventricular and septal weight; Kid, kidney weight; SBP, systolic blood pressure; UNaV, urinary sodium excretion. Data are mean±SD.

[a] $p<0.0001$ vs DR at the same period, * $p<0.05$ vs DR, ** $p<0.01$ vs DR.

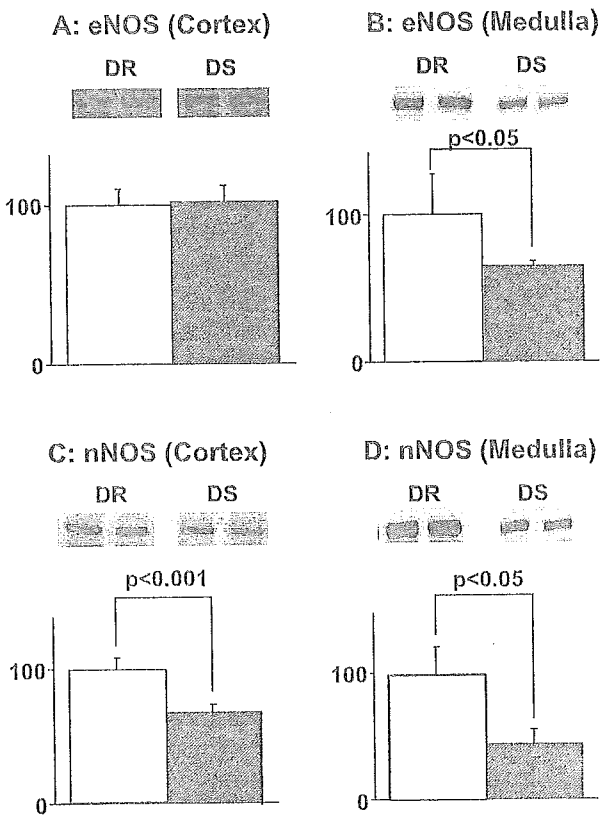

Fig. 1. Representative Western blots showing NOS and relative abundance of NOS in the renal cortex and medulla at the end of the 4th-week in Dahl rats in protocol 1 (n=4, in each group). A, B: eNOS; C,D: nNOS.

cantly restored eNOS expression in the renal medulla and nNOS expression in the renal cortex and medulla in DS rats at the end of the 4th-week (Fig. 2). Furthermore, the levels of proteinuria were significantly higher in DS rats than DR rats during all over the high sodium diet and chronic adrenomedullin infusion significantly inhibited the increasing of proteinuria levels under the high sodium diet in DS rats (Table 4). The immunohistochemical analysis revealed

Table 3
Number, body weight, heart rate, heart and kidney weights in Dahl rats treated with saline or adrenomedullin at the end of the 4th-week

	DR-S	DS-S	DS-AM
N	19	14	14
BW (g)	370±11	348±15*	350±14*
HR (bpm)	347±32	355±38	332±35
LV+SEP/BW (mg/g)	1.90±0.13	2.54±0.13*	2.32±0.14[a,*]
Kid/BW (mg/g)	3.85±0.28	4.63±0.26*	4.52±0.27*
SBP (mmHg)	128±6	173±10**	150±10[b,**]
UNaV (mmol/day)	2.2±0.7	1.4±0.5*	1.7±0.5

Abbreviations as in Table 1. DR-S indicates DR rats treated with saline; DS-S, DS rats treated with saline; DS-AM, DS rats treated with adrenomedullin. Data are mean±SD.

[a] p<0.001 vs DS-S.
[b] p<0.001 vs DS-S.
* p<0.001 vs DR-S.
** p<0.0001 vs DR-S.

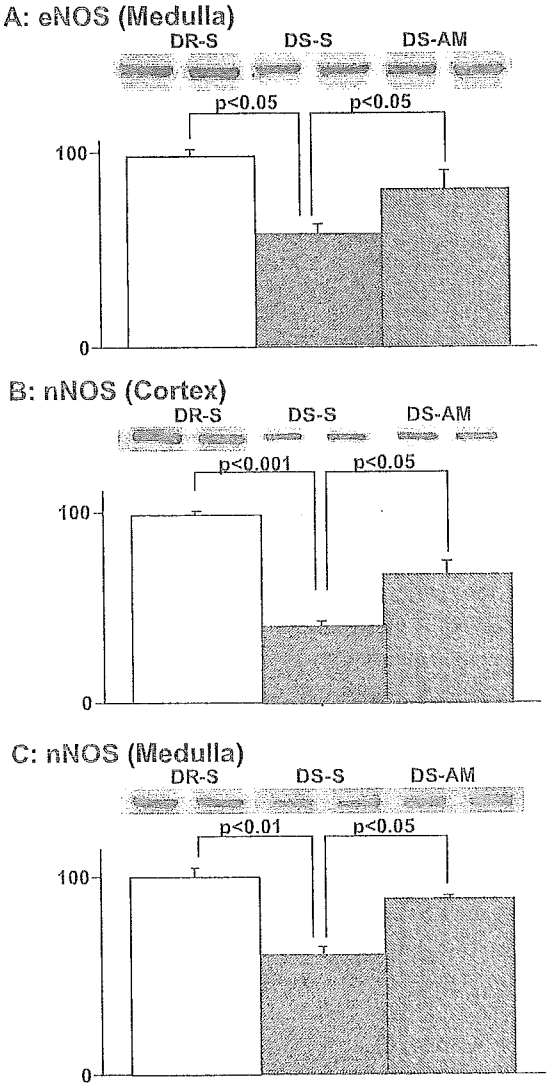

Fig. 2. The effect of chronic adrenomedullin infusion on the NOS expression in the renal cortex and medulla at the end of the 4th-week in protocol 2 (n=4, in each group). A: eNOS; B,C: nNOS.

that nNOS was localized in the macula densa and inner medullary collecting duct cells in all groups (Fig. 3).

4. Discussion

In the present study, we demonstrated for the first time that 1) the tissue adrenomedullin levels in the renal cortex and medulla significantly increased in DS rats compared with DR rats after 3 weeks on a high sodium diet, and were negatively correlated with urinary sodium excretion and positively correlated with systolic blood pressure, 2) the expression of eNOS in the renal medulla and nNOS in the renal cortex and medulla significantly reduced in DS rats, 3) chronic adrenomedullin supplementation significantly reduced systolic blood pressure, tended to increase urinary sodium excretion, and reduced urinary protein excretion in association with the restoration of renal medullary eNOS

Table 4
The effect of chronic adrenomedullin infusion on the levels of proteinuria during feeding on the high sodium diet in DS rats in protocol 2

Urinary protein (mg/day/100gBW)	2nd-week	3rd-week	4th-week
DR-S	3.4±1.1	3.2±0.9	3.4±0.9
DS-S	5.2±1.7*	6.5±2.5**	7.8±2.7**
DS-AM	3.5±1.0[b]	4.5±1.2[b]	5.7±1.6[a]

[a] $p<0.05$ vs DS-S.
[b] $p<0.01$ vs DS-S.
* $p<0.01$ vs DR-S.
** $p<0.0001$ vs DR-S.

and cortical and medullary nNOS expression, and 4) adrenomedullin may stimulate renal nNOS level in the macula densa and inner medullary collecting duct. These results suggest that chronic adrenomedullin infusion has beneficial effects on this hypertension probably in part through increased eNOS expression in renal medulla and nNOS expression in macula densa and inner medullary collecting duct in DS rats and that renal adrenomedullin may serve as an endogenous protective mechanism against salt-sensitive hypertension.

Adrenomedullin infusion has been reported not only to reduce systemic blood pressure in spontaneously hypertensive rats [13] and healthy human subjects [14], but also to increase urinary sodium excretion in anesthetized normal dogs [15]. These results suggested that adrenomedullin may regulate systemic blood pressure and urinary sodium excretion. However, the involvement of adrenomedullin has not been reported in the reduction of urinary sodium excretion that causes salt-sensitive hypertension in Dahl rats. Since we showed that the increased level of renal adrenomedullin correlated both with systemic blood pressure and urinary sodium excretion, there is a possibility that renal adrenomedullin is involved in the modulation of salt-sensitive hypertension in DS rats. Furthermore, chronic adrenomedullin infusion attenuated the increase of blood pressure and heart weight, suggesting that increased renal adrenomedullin may serve as an endogenous protective mechanism against salt-sensitive hypertension.

NO has been shown to play an important role in various physiological processes in the kidney, including sodium and fluid reabsorption [16], renal hemodynamics [17] and tubuloglomerular feedback [18]. Endogenous NO is enzymatically produced from the conversion of the amino acid L-arginine to L-citrulline, a reaction that is catalyzed by NOS. Three different NOS isoforms have been identified; namely a nNOS, a eNOS, and an inducible (iNOS) isoform, which are differentially expressed throughout the kidney [19]. Previous report demonstrated that renal eNOS activity was comparable between DS and DR rats under the high sodium diet [5]. We also compared the expression of eNOS protein in renal medulla and cortex, respectively between DS and DR rats. In the renal cortex eNOS expression had no significant difference between DS and DR rats after the 3-week high sodium diet. It was almost a similar result with the above report [5]. However, in the renal medulla eNOS expression was significantly reduced in DS rats compared with DR rats. Taken together with the fact that the inhibition of NOS causes salt-sensitive hypertension, the reduced eNOS expression in the renal medulla may be involved in part

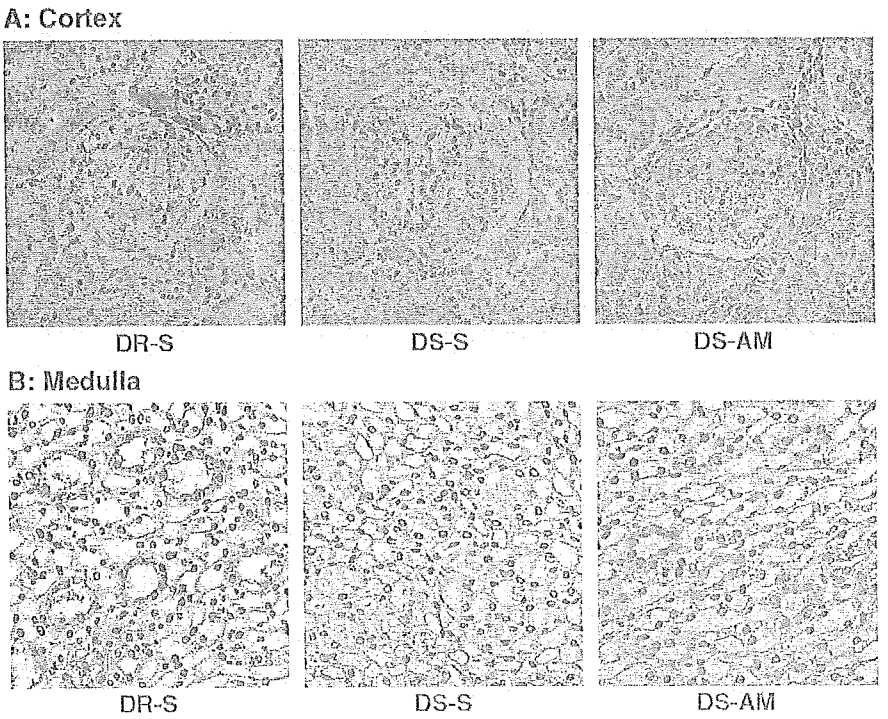

Fig. 3. Neuronal NOS immunoreactivity with a monoclonal antibody in the renal cortex and medulla at the end of the 4th-week in protocol 2.

in a reduction of urinary sodium excretion and an increase of blood pressure in DS rats. The expression of nNOS mRNA and immunoreactivity has been reported to exist in the macula densa and inner medullary collecting duct [19] in rats and renal nNOS specific activity was lower in DS rats than DR rats after a high sodium diet [5]. Interestingly, nNOS specific inhibition made the normally DR rats salt sensitive [20] and high sodium diet induced an increase in nNOS expression in the renal inner medulla of salt-resistant Sprague–Dawley rats [21]. Therefore, we evaluated the expression of nNOS. We observed a reduction in the nNOS level in the macula densa and inner medullary collecting duct in DS rats in the present Western blot and immunohistochemical analyses. Although we did not evaluate nNOS activity in the present study, our results suggested that one possible mechanism of salt-sensitive hypertension might be the reduced renal nNOS expression in the macula densa and inner medullary collecting duct in DS rats.

NO has been reported to be involved partly in vasodilation [22] and urinary sodium excretion [23] induced by adrenomedullin infusion. Recently, NO has been clarified to promote adrenomedullin gene expression in rat aortic vascular smooth muscle cells [24] and the maximal binding of adrenomedullin to its specific receptor in rat mesangial cells [25], suggesting that an accommodative interaction might exist between adrenomedullin and NO. Since we demonstrated that chronic adrenomedullin infusion attenuated salt-sensitive hypertension in association with the increased medullary eNOS expression and nNOS expression in the macula densa and inner medullary collecting duct, the attenuation of increasing of blood pressure by adrenomedullin infusion might be partly due to the increased eNOS and nNOS expression in the kidneys in DS rats.

In conclusion, our results suggest that chronic adrenomedullin infusion attenuates the increasing of blood pressure and decreases the degree of proteinuria probably in part through the increased renal medullary eNOS and nNOS expression in the macula densa and inner medullary collecting duct in DS rats and that renal adrenomedullin may serve as an endogenous protective mechanism against salt-sensitive hypertension. Our findings may open up the possibility of a new therapeutic strategy using adrenomedullin for salt-sensitive hypertension and renal injury.

Acknowledgements

Support for this study was provided in part by the Promotion of Fundamental Studies in Health Science of the Organization for Pharmaceutical Safety and Research (OPSR) of Japan, and by Grants-in-aid for Scientific Research (14571044) from Japan Society for the Promotion of the Science.

References

[1] Morimoto A, Uzu T, Fujii T, Nishimura M, Kuroda S, Nakamura S, et al. Sodium sensitivity and cardiovascular events in patients with essential hypertension. Lancet 1997;350:1734–7.
[2] Shultz PJ, Tolins JP. Adaptation to increased dietary salt intake in the rat. Role of endogenous nitric oxide. J Clin Invest 1993; 91:642–50.
[3] Baylis C, Harton P, Engels K. Endothelial derived relaxing factor controls renal hemodynamics in the normal rat kidney. J Am Soc Nephrol 1990;1:875–81.
[4] Tolins JP, Shultz PJ. Endogenous nitric oxide synthesis determines sensitivity to the pressor effect of salt. Kidney Int 1994; 46:230–6.
[5] Ikeda Y, Saito K, Kim JI, Yokohama M. Nitric oxide synthase isoform activities in kidney of Dahl salt-sensitive rats. Hypertension 1995;26:1030–4.
[6] Kitamura K, Kangawa K, Kawamoto M, Ichiki Y, Nakamura S, Matsuo H, et al. Adrenomedullin: a novel hypotensive peptide isolated from human pheochromocytoma. Biochem Biophys Res Commun 1993;192:553–60.
[7] Ichiki Y, Kitamura K, Kangawa K, Kawamoto M, Matsuo H, Eto T. Distribution and characterization of immunoreactive adrenomedullin in human tissue and plasma. FEBS Lett 1994;338:6–10.
[8] Jougasaki M, Wei C-M, Aarhus LL, Heublein DM, Sandberg SM, Burnett Jr JC. Renal localization and actions of adrenomedullin: a natriuretic peptide. Am J Physiol 1995;268:F657–63.
[9] Nishimatsu H, Suzuki E, Nagata D, Moriyama N, Satonaka H, Walsh K, et al. Adrenomedullin induces endothelium-dependent vasorelaxation via the phosphatidylinositol 3-kinase/Akt-dependent pathway in rat aorta. Circ Res 2001;89:63–70.
[10] Sakata J, Shimokubo T, Kitamura K, Nishizono M, Ichiki Y, Kangawa K, et al. Distribution and characterization of immunoreactive rat adrenomedullin in tissue and plasma. FEBS Lett 1994; 352:105–8.
[11] Gonick HC, Ding Y, Bondy SC, Ni Z, Vaziri ND. Lead-induced hypertension: interplay of nitric oxide and reactive oxygen species. Hypertension 1997;30:1487–92.
[12] Suga SI, Phillips MI, Ray PE, Raleigh JA, Vio CP, Kim YG, et al. Hypokalemia induces renal injury and alterations in vasoactive mediators that favor salt sensitivity. Am J Physiol Renal Physiol 2001;281:F620–9.
[13] Khan AI, Kato J, Kitamura K, Kangawa K, Eto T. Hypotensive effect of chronically infused adrenomedullin in conscious Wistar–Kyoto and spontaneously hypertensive rats. Clin Exp Pharmacol Physiol 1997;24:139–42.
[14] Lainchbury JG, Cooper GJ, Coy DH, Jiang NY, Lewis LK, Yandle TG, et al. Adrenomedullin: a hypotensive hormone in man. Clin Sci (Lond) 1997;92:467–72.
[15] Jougasaki M, Aarhus LL, Heublein DM, Sandberg SM, Burnett Jr JC. Role of prostaglandins and renal nerves in the renal actions of adrenomedullin. Am J Physiol 1997;272:F260–6.
[16] Kone BC, Baylis C. Biosynthesis and homeostatic roles of nitric oxide in the normal kidney. Am J Physiol 1997;272:F561–78.
[17] Kurtz A, Gotz KH, Hamann M, Sandner P. Mode of nitric oxide action on the renal vasculature. Acta Physiol Scand 2000;168:41–5.
[18] Ren YL, Garvin JL, Carretero OA. Role of macula densa nitric oxide and cGMP in the regulation of tubuloglomerular feedback. Kidney Int 2000;58:2053–60.
[19] Marsden PA, Hall AV, Brenner BM. Reactive nitrogen and oxygen intermediates and the kidney. In: Brenner BM, editor. The kidney, 5th ed. Philadelphia: WB Saunders; 1996. p. 719–21.
[20] Tan DY, Meng S, Manning Jr RD. Role of neuronal nitric oxide synthase in Dahl salt-sensitive hypertension. Hypertension 1999; 33:456–61.
[21] Mattson DL, Higgins DJ. Influence of dietary sodium intake on renal medullary nitric oxide synthase. Hypertension 1996;27:688–92.

[22] Hirata Y, Hayakawa H, Suzuki Y, Suzuki E, Ikenouchi H, Kohmoto O, et al. Mechanisms of adrenomedullin-induced vasodilation in the rat kidney. Hypertension 1995;25:790–5.
[23] Majid DS, Kadowitz PJ, Coy DH, Navar LG. Renal responses to intra-arterial administration of adrenomedullin in dogs. Am J Physiol 1996;270:F200–5.
[24] Hofbauer KH, Schoof E, Kurtz A, Sandner P. Inflammatory cytokines stimulate adrenomedullin expression through nitric oxide-dependent and-independent pathways. Hypertension 2002;39:161–7.
[25] Dotsch J, Schoof E, Schocklmann HO, Brune B, Knerr I, Repp R, et al. Nitric oxide increases adrenomedullin receptor function in rat mesangial cells. Kidney Int 2002;61:1707–13.